Contribution from the Departments of Chemistry, State University of New York at Albany, Albany, New York 12222, and Syracuse University, Syracuse, New York 13244

Preparations, Structures, and Reactions of Molybdenum Complexes of Triorgano Silylated Pyridine-2-thiols

Eric Block,*,† Michael Gernon,† Hyunkyu Kang,‡ Gabriel Ofori-Okai,† and Jon Zubieta*,‡

Received July 27, 1990

Reactions of molybdenum halide precursors with 3-(trimethylsilyl)pyridine-2-thiol (**1**) or 3,6-bis(*tert*-butyldimethylsilyl)-pyridine-2-thiol (**2**) yield a variety of mononuclear and binuclear Mo(III) and Mo(IV) complexes depending on reaction conditions. Illustrative of these classes of complexes are the species $[MoCl_4(2\text{-}SC_5H_3NH\text{-}3\text{-}SiMe_3)_2]$ (**3**), $[MoCl_3\{2\text{-}SC_5H_2NH\text{-}3,6\text{-}(SiMe_2Bu^t)_2\}_3]$ (**4**), $[MoCl_4\{2\text{-}SC_5H_2NH\text{-}3,6\text{-}(SiMe_2Bu^t)_2\}_2]\cdot(C_2H_5)_2O$ (**6**), $(Ph_4P)[MoBr_4(2\text{-}SC_5H_3NH\text{-}3\text{-}SiMe_3)_2]$ (**7**), and $[MoBr_3(2\text{-}SC_5H_3NH\text{-}3\text{-}SiMe_3)_3]$ (**8**). Reactions of **3** with molecular oxygen in excess and in stoichiometric quantities yield $[Mo_2O_3(2\text{-}SC_5H_3N\text{-}3\text{-}SiMe_3)_4$ (**9**) and $[MoOCl(2\text{-}SC_5H_3N\text{-}3\text{-}SiMe_3)_2]$ (**10**), respectively. In contrast, **7** reacts with O_2 to yield $(Ph_4P)[MoOBr_3(2\text{-}SC_5H_3N\text{-}3\text{-}SiMe_3)]$ (**11**). Organohydrazine ligands react with **3** by halide displacement and formal oxidation to yield the Mo(VI) species $[MoCl_2(2\text{-}SC_5H_3N\text{-}3\text{-}SiMe_3)_2(NNMePh)]$ (**12**) and $[Mo(NNMePh)_2(2\text{-}SC_5H_3N\text{-}3\text{-}SiMe_3)_2]$ (**13**). Complex **12** exhibits a seven-coordinate pentagonal-bipyramidal geometry similar to that of $[Mo(NNMePh)(SC_6H_4PPhC_6H_4S)_2]$ (**17**). Reductions of **3** and **6** with hydrazine yield the binuclear Mo(III) complexes $[Mo_2Cl_6(2\text{-}SC_5H_3NH\text{-}3\text{-}SiMe_3)_3]\cdot 2CH_3CN$ (**14**) and $[Mo_2Cl_6\{(2\text{-}SC_5H_2NH\text{-}3,6\text{-}(SiMe_2Bu^t)_2\}_3]$ (**15**), respectively. Crystal data: **4**, monoclinic $P2_1/n$, a = 17.644 (5) Å, b = 17.067 (5) Å, c = 25.798 (5) Å, β = 99.17 (1)°, V = 7669.8 (11) Å^3, Z = 4, 2472 reflections, R = 0.089; **6**, orthorhombic *Pcan*, a = 16.245 (5) Å, b = 13.531 (4) Å, c = 23.739 (7) Å, V = 5218.4 (12) Å^3, Z = 4, 1533 reflections, R = 0.073; **7**, triclinic $P\bar{1}$, a = 10.689 (1) Å, b = 14.511 (3) Å, c = 16.713 (3) Å, α = 104.15 (1)°, β = 103.58 (1)°, γ = 95.46 (1)°, V = 2411.6 (8) Å^3, Z = 2, 3510 reflections, R = 0.053; **8**, orthorhombic, *Pbca*, a = 33.376 (6) Å, b = 18.751 (4) Å, c = 11.980 (4) Å, V = 7494.6 (13) Å^3, Z = 8, 2864 reflections, R = 0.032; **9**, monoclinic $P2_1/c$, a = 11.719 (4) Å, b = 14.258 (7) Å, c = 14.081 (3) Å, β = 99.91 (2)°, V = 2317.8 (11) Å^3, Z = 2, 1571 reflections, R = 0.086; **10**, monoclinic $P2_1/c$, a = 12.858 (3) Å, b = 13.655 (3) Å, c = 13.290 (3) Å, β = 96.67 (2)°, V = 2317.7 (12) Å^3, Z = 4, 1843 reflections, R = 0.083; **11**, monoclinic $C2/c$, a = 19.806 (4) Å, b = 12.271 (3) Å, c = 32.749 (5) Å, β = 96.57 (1)°, V = 7907.4 (12) Å^3, Z = 8, 2440 reflections, R = 0.083; **12**, monoclinic $P2_1/c$, a = 10.727 (3) Å, b = 16.428 (5) Å, c = 22.800 (6) Å, β = 97.67 (2)°, V = 3981.9 (21) Å^3, Z = 4, 2299 reflections, R = 0.072; **13**, monoclinic $C2/c$, a = 22.833 (5) Å, b = 10.731 (2) Å, c = 14.645 (4) Å, β = 102.25 (1)°, V = 3506.9 (21) Å^3, Z = 4, 2402 reflections, R = 0.051; **14**, triclinic $P\bar{1}$, a = 10.605 (3) Å, b = 13.277 (4) Å, c = 16.969 (5) Å, α = 79.82 (1)°, β = 84.19 (2)°, γ = 71.51 (1)°, V = 2228.0 (11) Å^3, Z = 2, 2249 reflections, R = 0.053; **15**, orthorhombic *Pbca*, a = 15.338 (4) Å, b = 30.447 (8) Å, c = 33.913 (8) Å, V = 15838.2 (27) Å^3, Z = 8, 5163 reflections, R = 0.059; **17**, monoclinic $P2_1/n$, a = 13.466 (2) Å, b = 15.023 (2) Å, c = 21.565 (3) Å, β = 100.05 (1)°, V = 4296.9 (12) Å^3, Z = 4, 4337 reflections, R = 0.038.

Although metal thiolates have been known from the very beginnings of coordination chemistry, the last two decades have witnessed a dramatic increase in the reported chemistry of these species,[1-3] primarily as a consequence of the observation that thiolate coordination occurs for many metal ions in metalloenzymes. Recent work has demonstrated that sterically hindered thiolate ligands afford complexes with unusual geometries[4-10] or oxidation states[11,12] and enhanced solubilities. Furthermore, by regulation of the degree of steric hindrance, the microenvironment of the metal may be modified to allow reaction with substrate molecules.[13-19] We have shown that silicon is a useful structural element in thiolate ligands in complexes involving silylated methanethiols[20] and benzenethiols[21] and by functioning as a connector in the synthesis of dithiols,[20] such as bis(mercaptomethyl)dimethylsilane and bis(mercaptophenyl)dimethylsilane. More recently, we have extended these studies to syntheses of complexes of 3-(triorganosilyl)pyridine-2-thiols (A) and 3,6-bis(triorganosilyl)pyridine-2-thiols (B).[22,23]

As illustrated in Chart I, the ligand pyridine-2-thiol may coordinate as the conjugate anion, pyridine-2-thiolate (pyS$^-$), or in the 1*H*-pyridine-2-thione form (C).[24-30] The pyridine-2-thiolato ligand is commonly monodentate through the S donor (D)[31,32] or bidentate through the S and N donors (E),[33-39] although bridging modes through both heteroatoms (F)[39-42] or exclusively through the thiolate donor (G)[43] may be adopted. In addition, the ligand may function as a five-electron donor in the μ_3 modes H[39,43,44] and I.[45] The chemistry of the silylated pyridine-2-thiol ligands has been largely limited to complexes of Cu, Ag, and Hg where coordination types D and F are observed. In this paper,[46] we extend the coordination chemistry of silylated pyridine-2-thiols to molybdenum and report on the synthesis and structural characterization of a series of novel mononuclear molybdenum–halido–(1*H*-pyridine-2-thione) complexes and their reactions with molecular oxygen, hydrazine and organohydrazines. The structures of $[MoCl_4\{SC_5H_2NH\text{-}3,6\text{-}(SiMe_2Bu^t)_2\}_2]$ (**4**), $(Ph_4P)[MoBr_4(SC_5H_3NH\text{-}3\text{-}SiMe_3)_2]$ (**6**), $[MoBr_3(SC_5H_3NH\text{-}3\text{-}$

Chart I. Novel Sterically Hindered Thiol Ligand Types A and B and Representations of Coordination Modes Described for the Pyridine-2-thiol Ligand (C–I)

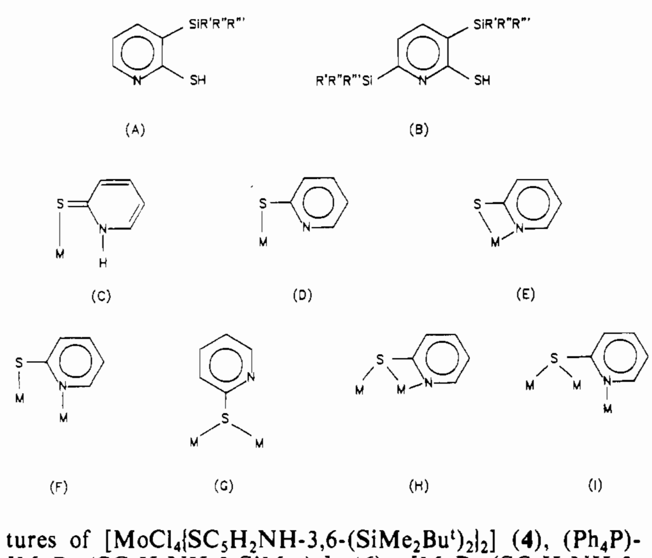

† State University of New York at Albany.
‡ Syracuse University.

(1) Muller, A.; Diemann, E. In *Comprehensive Coordination Chemistry*; Wilkinson, G., Ed.; Pergamon Press: Oxford, England, 1987; Vol. 2, p 515.
(2) Dance, I. G. *Polyhedron* **1986**, *5*, 1037.
(3) Blower, P. G.; Dilworth, J. R. *Coord. Chem. Rev.* **1987**, *76*, 121.
(4) Gruff, E. S.; Koch, S. A. *J. Am. Chem. Soc.* **1990**, *112*, 1245.
(5) Bishop, P. T.; Blower, P. J.; Dilworth, J. R.; Zubieta, J. *Polyhedron* **1986**, *5*, 363.
(6) Bishop, P. T.; Dilworth, J. R.; Zubieta, J. A. *J. Chem. Soc., Chem. Commun.* 1985, 257.
(7) Bishop, P. T.; Dilworth, J. R.; Nicholson, T.; Zubieta, J. A. *J. Chem. Soc., Chem. Commun.* **1986**, 1123.
(8) Fikar, R.; Koch, S. A.; Millar, M. M. *Inorg. Chem.* **1985**, *24*, 3311.
(9) Roland, E.; Walborsky, E. C.; Dewan, J. C.; Schrock, R. R. *J. Am. Chem. Soc.* **1985**, *107*, 5795.

0020-1669/91/1330-1736$02.50/0

$SiMe_3)_3$] (7), and $(Ph_4P)[MoOBr_3(SC_5M_3N\text{-}3\text{-}SiMe_3)]$ (10) have been described briefly in a previous communication.[96]

(10) Listemann, M. L.; Dewan, J. C.; Schrock, R. R. *J. Am. Chem. Soc.* **1985**, *107*, 7207.
(11) Koch, S. A.; Millar, M. M. *J. Am. Chem. Soc.* **1983**, *105*, 3362.
(12) Millar, M. M.; O'Sullivan, T.; deVries, N. *J. Am. Chem. Soc.* **1985**, *107*, 3714.
(13) Blower, P. J.; Dilworth, J. R.; Hutchinson, J.; Nicholson, T.; Zubieta, J. A. *J. Chem. Soc. Dalton Trans.* **1985**, 2639.
(14) Blower, P. J.; Dilworth, J. R.; Zubieta, J. A. *J. Chem. Soc., Dalton Trans.* 1985, 1533.
(15) Millar, M.; Koch, S. A.; Fikar, R. *Inorg. Chim. Acta* **1984**, *88*, L15.
(16) Caradonna, J. P.; Reddy, P. R.; Holm, R. H. *J. Am. Chem. Soc.* **1988**, *110*, 2139 and references therein.
(17) Kamata, M.; Yoshida, T.; Otsuka, S. *J. Am. Chem. Soc.* **1981**, *103*, 3574.
(18) Kamata, M.; Hirotsu, K.; Higuchi, T.; Kido, M.; Tatsumi, K.; Yoshida, T.; Otsuka, S. *Inorg. Chem.* **1983**, *22*, 2416.
(19) Walborsky, E. C.; Wigley, D. E.; Roland, E.; Dewan, J. C.; Schrock, R. R. *Inorg. Chem.* **1987**, *26*, 1615.
(20) Block, E.; Aslam, M. *Tetrahedron Lett.* **1985**, *26*, 2259. Aslam, M.; Bartlett, R. A.; Block, E.; Olmstead, M. M.; Power, P. P.; Siegel, G. E. *J. Chem. Soc., Chem. Commun.* **1985**, 1674. Block, E.; Aslam, M. *J. Am. Chem. Soc.* **1985**, *107*, 6729. Tang, K.; Aslam, M.; Block, E.; Nicholson, T.; Zubieta, J. *Inorg. Chem.* **1987**, *26*, 488. Koo, B.-K.; Block, E.; Liu, S.; Zubieta, J. *Polyhedron* **1988**, *7*, 1397.
(21) Block, E.; Gernon, M.; Kang, H.; Liu, S.; Zubieta, J. *J. Chem. Soc., Chem. Commun.* **1988**, 1031. Block, E.; Eswarakrishnan, V.; Gernon, M.; Ofori-Okai, G.; Saha, C.; Tang, K.; Zubieta, J. *J. Am. Chem. Soc.* **1989**, *111*, 658. Block, E.; Kang, H.; Ofori-Okai, G.; Zubieta, J. *Inorg. Chim. Acta* **1989**, *156*, 27. Block, E.; Gernon, M.; Kang, H.; Ofori-Okai, G.; Zubieta, J. *Inorg. Chem.* **1989**, *28*, 1263. Block, E.; Ofori-Okai, G.; Zubieta, J. *J. Am. Chem. Soc.* **1989**, *111*, 2327. Block, E.; Kang, H.; Ofori-Okai, G.; Zubieta, J. *Inorg. Chim. Acta* **1990**, *166*, 155. Block, E.; Kang, H.; Ofori-Okai, G.; Zubieta, J. *Inorg. Chim. Acta* **1990**, *167*, 147.
(22) Block, E.; Gernon, M.; Kang, H.; Zubieta, J. *Angew. Chem., Int. Ed. Engl.* **1988**, *27*, 1342.
(23) Block, E.; Brito, M.; Gernon, M.; McGowty, D.; Kang, H.; Zubieta, J. *Inorg. Chem.* **1990**, *29*, 3172.
(24) Kennedy, B. P.; Lever, A. B. P. *Can. J. Chem.* **1972**, *50*, 3488.
(25) Binamira-Soriaga, E.; Lundeen, M.; Seff, K. *Acta Crystallogr., Sect. B* **1979**, *B35*, 2875.
(26) Deeming, A. J.; Hardcastle, K. I.; Meah, M. N.; Bates, P. A.; Dawes, H. M.; Hursthouse, M. B. *J. Chem. Soc., Dalton Trans.* **1988**, 227.
(27) Kokkou, S. C.; Rentzeperis, P.; Karagiannides, P. *Acta Crystallogr., Sect. C* **1983**, *C39*, 178. Kokkou, S. C.; Schramm, V.; Karagiannidis, P. *Acta Crystallogr.*, **1985**, *C41*, 1040.
(28) Valle, G.; Ettore, R.; Vettori, U.; Peruzzo, V.; Plazzogna, G. *J. Chem. Soc., Dalton Trans.* **1987**, 818.
(29) Raper, E. S. *Coord. Chem. Rev.* **1985**, *61*, 115.
(30) Broomhead, J. A.; Greenwood, R.; Pienkowski, W.; Sterns, M. *Aust. J. Chem.* **1986**, *36*, 1895.
(31) Mura, P.; Olby, B. G.; Robinson, S. D. *J. Chem. Soc., Dalton Trans.* **1985**, 2101 and references therein.
(32) Deeming, A. J.; Meah, N. M. *Inorg. Chim. Acta* **1986**, 117, L13.
(33) Rosenfield, S. G.; Berends, H. P.; Gelmini, L.; Stephan, D. W.; Mascharak, P. K. *Inorg. Chem.* **1987**, *26*, 2792.
(34) Mura, P.; Robinson, S. D. *Acta Crystallogr., Sect. C* **1984**, *C40*, 1798.
(35) Mura, P.; Olby, B. G.; Robinson, S. D. *Inorg. Chim. Acta* **1985**, *98*, L21.
(36) Nagaraja, K. S.; Udupa, M. R. *Bull. Chem. Soc. Jpn.* **1984**, *57*, 1705.
(37) Cotton, F. A.; Fanwick, P. E.; Fitch, J. W., III. *Inorg. Chem.* **1978**, *17*, 3254.
(38) Rosenfield, S. G.; Swedberg, S. A.; Arora, S. K.; Mascharak, P. K. *Inorg. Chem.* **1986**, *25*, 2109.
(39) Deeming, A. J.; Meah, M. N.; Dawes, H. M.; Hursthouse, M. B. *J. Organomet. Chem.* **1986**, *299*, C25.
(40) Ciriano, M. A.; Viguri, F.; Ora, L. A.; Tiripicchio, A.; Tiripicchio-Camellini, M. *Angew. Chem., Int. Ed. Engl.* **1987**, *26*, 444.
(41) Zhang, N.; Wilson, S. R.; Shapley, P. A. *Organometallics* **1988**, *7*, 1126.
(42) Umakoshi, K.; Kinoshuta, I.; Ichimura, A.; Ooi, S. *Inorg. Chem.* **1987**, *26*, 3551.
(43) Oro, L. A.; Ciriano, M. A.; Viguri, F.; Tiripicchio, A.; Tiripicchio-Camellini, M.; Lahoz, F. J. *Nouv. J. Chim.* **1986**, *10*, 75.
(44) Deeming, A. J.; Meah, M. N.; Bates, P. A.; Hursthouse, M. B. *J. Chem. Soc., Dalton Trans.* **1988**, 235.
(45) Deeming, A. J.; Karin, M.; Bates, P. A.; Hursthouse, M. B. *Polyhedron* **1988**, *7*, 1401.

Experimental Section

All manipulations were carried out under purified Ar by using standard Schlenk techniques. All solvents were dried and rigorously deoxygenated prior to use. The following instruments were used in this work: IR spectra, Perkin-Elmer 283B infrared spectrophotometer; ^{1}H NMR spectra, Varian 300XL spectrometer; UV/visible spectra, Shimadzo Model UV-160 spectrophotometer; X-ray crystallography, Nicolet R3mV diffractometer; electrochemical investigations, BAS 100 electroanalytical system using a solution 3×10^{-3} M in complex in 0.1 M $(n\text{-}Bu_4N)(PF_6)$; EPR measurements, Varian E4 spectrometer. $[Mo_2Br_4(CO)_8]$ was prepared by literature methods,[47] as was $[MoCl_4(CH_3CN)_2]$.[48]

Pyridine-2-thiol (1). A modified literature procedure[49] was used. 2-Chloropyridine (113.0 g, 1.0 mol) thiourea (84.1 g, 1.0 mol), and ethanol (300 mL) were mixed and refluxed for 4 h and then treated with aqueous ammonia (150 mL). The solution was allowed to stand at room temperature for 5 days whereupon the volatiles were removed at 100 °C and under aspirator pressure. The title compound was obtained as yellow needles from benzene (44.4 g, 40% yield): mp 124–126 °C [lit.[49] mp 124–126 °C]; ^{1}H NMR δ 7.63 (d, 1 H, J = 6.4 Hz), 7.58 (d, 1 H, J = 8.9 Hz), 7.42 (dd, 1 H, J = 8.9, 7.8 Hz), 6.81 (dd, 1 H, J = 7.8, 6.4 Hz); ^{13}C NMR δ 176.72, 137.97, 136.86, 133.81, 114.07; IR (KBr) 2900, 1580, 1500, 1440, 1365, 1140, 980, 740 cm^{-1}; GC–MS m/e 111 (M^+, 100%), 67 (85%).

3-(Trimethylsilyl)pyridine-2-thiol (1a). A solution of pyridine-2-thiol (22.2 g, 0.20 mol) in dry THF (300 mL) was added slowly under argon to a stirred THF solution of LDA at 0 °C prepared from Pr^i_2NH (61 g, 0.600 mol) and 2.5 M *n*-butyllithium (250 mL, 0.620 mol). The solution was stirred at 0 °C for 2, treated with chlorotrimethylsilane (87.0 g, 0.80 mol), and stirred at room temperature for 12 h. The reaction was quenched with water (5 mL) and then concentrated in vacuo. The crude product was neutralized (pH adjusted to pH 5–8) with 5% HCl and saturated NH_4Cl, and the organic products were extracted with CH_2Cl_2 (2 × 600 mL). The combined organic phase was washed once with water, dried with $MgSO_4$, and concentrated in vacuo to yield a crude yellow solid. The crude solid was washed with a small amount of pentane and recrystallized from benzene to yield the title compound as a yellow solid (20.0 g 55% yield): mp 194–195 °C [after sublimation at 110 °C (0.5 Torr)]; ^{1}H NMR d 7.59 (d, 1 H, J = 7.2 Hz), 7.56 (d, 1 H, J = 6.4 Hz), 6.76 (dd, 1 H, J = 7.2, 6.4 Hz), 0.42 (s, 9 H); ^{13}C NMR δ 181.00, 144.55, 144.10, 137.13, 113.57, −1.31; IR (KBr) 2900, 1570, 1300, 1150, 1010, 730 cm^{-1}; GC–MS m/e 183 (M^+, 14%), 168 (100%). Anal. Calcd for $C_8H_{13}SNSi$: C, 52.41; H, 7.15; N, 7.64. Found: C, 52.37; H, 7.02; N, 7.56.

3-(Triethylsilyl)pyridine-2-thiol (1b). A mixture of LDA (0.04 mol), pyridine-2-thiol (1.1 g, 0.01 mol), and THF (100 mL) was treated with bromotriethylsilane (5.9 g, 0.30 mol) and stirred at room temperature for 24 h. Workup as above produced **1b** as a yellow solid (1.0 g, 45% yield): mp 135–136 °C [after sublimation at 130 °C (0.1 torr)]; ^{1}H NMR δ 7.56–7.42 (m, 2 H), 6.74 (dd, 1 H, J = ca. 6.6 Hz), 1.07–0.92 (m, 15 H); ^{13}C NMR δ 181.35, 145.80, 141.71, 137.02, 113.31, 7.54, 2.67; IR (KBr) 2900, 2500, 1610, 1570, 1310, 1140, 1010, 730 cm^{-1}; GC–MS m/e 225 (M^+, 3%), 196 (100%), 168 (33%), 140 (37%). Anal. Calcd for $C_{11}H_{19}SNSi$: C, 58.61; H, 8.50; N, 6.21. Found: C, 58.77; H, 8.51; N, 6.28.

3,6-Bis(*tert*-butyldimethylsilyl)pyridine-2-thiol (1c). In a procedure identical with that used to prepare **1a**, the mixture of LDA (0.10 mol), pyridine-2-thiol (3.33 g, 0.03 mol), and THF (160 mL) was treated with chloro-*tert*-butyldimethylsilane (15.0 g, 0.10 mol) and stirred at room temperature for 48 h.

Workup as above yielded **1c** as a yellow solid (5.59 g, 55% yield); mp 174–175 °C [after sublimation at 165 °C (0.1 torr)]; ^{1}H NMR d 10.4 (br s, 1 H), 7.46 (d, 1 H, J = 6.8 Hz), 6.72 (d, 1 H, J = 6.8 Hz), 1.00 (s, 9 H), 0.95 (s, 9 H), 0.41 (s, 6 H), 0.33 (s, 6 H); ^{13}C NMR δ 184.58, 152.52, 143.94, 142.69, 119.84, 27.90, 26.24, 18.32, 16.87, −3.80, −7.16; IR (KBr, cm^{-1}) 2950, 1570, 1550, 1470, 1290; GC–MS m/e 339 (M^+, 4%), 282 (100%), 224 (57%), 210 (21%), 73 (38%), 57 (42%). Anal. Calcd for $C_{17}H_{33}NSi_2S$: C, 60.11; H, 9.79; N, 4.12. Found: C, 59.91; H, 9.97; N, 4.07.

3-(Dimethylphenylsilyl)pyridine-2-thiol (1d). In a procedure identical with that used to prepare **2**, the mixture of LDA (0.18 mol), pyridine-2-thiol (6.66 g, 0.06 mol), and THF (200 mL) was treated with chloro-

(46) The work presented in this paper is discussed in the following doctoral dissertations: Gernon, M. Doctoral Dissertation, State University of New York at Albany, 1989. Kang, H. Doctoral Dissertation, State University of New York at Albany, 1990.

(47) Colton, R.; Rix, E. J. *Aust. J. Chem.* **1969**, *22*, 305.
(48) Allen, E. A.; Brisdon, B. J.; Fowles, G. W. A. *J. Chem. Soc.* **1964**, 4531.
(49) Jones, R. A.; Katritzky, A. R. *J. Chem. Soc.* **1958**, 3610.

dimethylphenylsilane (24.0 g, 0.14 mol) and stirred at room temperature for 24 h. Workup as above produced **1d** as a yellow solid (4.4 g, 30% yield): mp 161–162 °C [after sublimation at 150 °C (0.1 mm)]; ^{1}H NMR δ 7.61–7.58 (m, 2 H), 7.46 (dd, 1 H, *J* = 6.5, 2.1 Hz), 7.38–7.35 (m, 3 H), 7.32 (dd, 1 H, *J* = 7.6, 2.1 Hz), 6.61 (t, 1 H, *J* = 6.6 Hz), 0.74 (s, 6 H); ^{13}C NMR δ 181.09, 146.00, 142.54, 137.57, 137.46, 134.42, 129.11, 127.84, 113.40, −2.79; IR (KBr, cm^{-1}) 2850, 1605, 1580, 1430, 1305, 1150; GC–MS m/e 245 (M$^+$, 21%), 230 (70%), 196 (39%), 168 (100%), 167 (97%), 152 (39%). Anal. Calcd for $C_{13}H_{15}NSSi$: C, 63.62; H, 6.16; N, 5.71. Found: C, 63.58; H, 6.14; N, 5.66.

3,6-Bis(*tert*-butyldiphenylsilyl)pyridine-2-thiol (1e). A mixture of LDA (0.05 mol), pyridine-2-thiol (1.11 g, 0.01 mol), and THF (80 mL) was treated with chloro-*tert*-butyldiphenylsilane (10.0 g, 0.036 mol) and stirred at room temperature for 48 h. Workup as above followed by recrystallization from CH_2Cl_2 and radial chromatography (silica gel, 1:1 hexane–CH_2Cl_2) yielded **1e** as a yellow solid (2.2 g, 37% yield); mp 193–194 °C; ^{1}H NMR δ 10.4 (br s, 1 H), 7.60, −7.30 (m, 21 H), 6.85 (d, 1 H, *J* = 6.7 Hz), 1.33 (s, 9 H), 1.22 (s, 9 H); ^{13}C NMR δ 185.34, 150.45, 146.83, 141.33, 137.17, 136.11, 134.96, 130.81, 129.71, 128.94, 128.70, 127.56, 121.25, 30.65, 28.43, 19.08, 18.84; IR (KBr, cm^{-1}) 3325, 2950, 1540, 1430, 1295, 1150, 1140, 1110, 740, 700; MS m/e 587 (M$^+$). Anal. Calcd for $C_{37}H_{41}NSi_2S$: C, 75.58; H, 7.03; N, 2.38. Found: C, 76.01; H, 6.97; N, 2.43.

3,6-Bis(triisopropylsilyl)pyridine-2-thiol (1f). A mixture of LDA (0.04 mol), pyridine-2-thiol (1.11 g, 0.01 mol), and THF (100 mL) was treated with chlorotriisopropylsilane (9.6 g, 0.050 mol) and allowed to stir at room temperature for 24 h. Workup as above followed by radial chromatography (silica gel–pentane, CH_2Cl_2 gradient) yielded **1f** as a yellow solid (0.54 g, 20% yield): mp 178–180 °C; ^{1}H NMR δ 7.48 (d, 1 H, *J* = 6.8 Hz), 6.70 (d, 1 H, *J* = 6.8 Hz), 1.79 (septet, 3 H, *J* = 8.0 Hz), 1.35 (septet, 3 H, *J* = 6.0 Hz), 1.13 (d, 18 H, *J* = 6.0 Hz), 1.10 (d, 18 H, *J* = 8.0 Hz); ^{13}C NMR δ 184.91, 150.47, 144.14, 141.26; 120.36; IR (KBr) 2946, 2865, 2362, 2344, 1541, 1458, 1281, 1157, 1128, 1018, 881, 779, 668, 652 cm^{-1}.

6-(*tert*-Butyldimethylsilyl)pyridine-2-thiol (1g). A mixture of LDA (0.05), pyridine-2-thiol (2.22 g, 0.02 mol), and THF (100 mL) was treated with chloro-*tert*-butyldimethylsilane (7.5 g, 0.05 mol) and stirred at room temperature for 24 h. Workup as above yielded a 1/1 mixture of **1g** and **1a**. The compound **1g** was obtained as a pure yellow solid following radial chromatography (silica gel–hexane, CH_2Cl_2 gradient, 1.36 g, 30% yield, 60% yield based on unrecovered starting material): mp 105–106 °C [after sublimation at 100 °C (0.1 mm)]; ^{1}H NMR δ 7.53 (d, 1 H, *J* = 8.8 Hz), 7.25 (dd, 1 H, *J* = 8.8, 6.8 Hz), 6.77 (d, 1 H, *J* = 6.8 Hz), 0.95 (s, 9 H), 0.35 (s, 6 H); ^{13}C NMR δ 180.10, 152.49, 135.42, 134.04, 120.73, 26.21, 16.87, −7.03; IR (KBr, cm^{-1}) 3179, 2952, 2928, 2895, 2858, 1583, 1564, 1467, 1365, 1259, 1149, 1128, 981, 836, 773, 708; GC–MS m/e 225 (M$^+$, 11%), 168 (100%), 154 (14%), 115 (17%). Anal. Calcd for $C_{11}H_{18}SiNS$: C, 58.61; H, 8.50; N, 6.21. Found: C, 58.66; H, 8.41; N, 6.24.

3-(Trimethylsilyl)-6-(triethylsilyl)pyridine-2-thiol (1h). The mixture of LDA (0.10 mol), 3-(trimethylsilyl)-2-mercaptopyridine (5.5 g, 0.03), and THF (150 mL) was treated with chlorotriethylsilane (15.0 g, 0.10 mol) and allowed to stir at room temperature for 24 h. Workup as above followed by radial chromatography (silica gel–hexane) and recrystallization from hexane gave **1h** as a yellow solid (2.5 g, 28% yield): mp 126–127 °C [after sublimation at 120 °C (0.1 mm)]; ^{1}H NMR 10.7 (br s, 1 H), 7.44 (d, 1 H, *J* = 6.5 Hz), 6.75 (dd, 1 H, *J* = 6.5, 2.5 Hz), 1.00 (t, 9 H, *J* = 7.4 Hz), 0.86 (q, 6 H, *J* = 7.4 Hz), 0.40 (s, 9 H); ^{13}C NMR δ 183.98, 152.40, 144.10, 142.35, 120.32, 7.04, 2.32, −1.39; IR (KBr, cm^{-1}) 3120, 3000, 2850, 2800, 1580, 1560, 1300, 1250, 1160, 875, 860, 740; GC–MS *m/e* 297 (M$^+$, 34%), 282 (100%), 252 (42%), 224 (27%), 196 (38%), 73 (26%), 59 (33%). Anal. Calcd for $C_{14}H_{27}Si_2SN$: C, 56.50; H, 9.15; N, 4.71. Found: C, 56.60; H, 9.03; N, 4.65.

Bis(2-mercaptophenyl)phenylphosphine (2). Solvents used to isolate product were degassed and saturated with argon. Lithium 2-lithiobenzenethiolate was prepared as described elsewhere[95] from thiophenol (7 g, 0.064 mol), TMEDA (22 mL, 0.142 mol), and 2.5 M *n*-butyllithium in hexane (57 mL, 0.142 mol). Solid lithium 2-lithiobenzenethiolate was isolated by filtration under argon on a Schlenk frit, washed with dry hexane (2 × 50 mL), and dissolved in dry THF (100 mL) precooled to −78 °C. A stirred solution of 2-lithiobenzenethiolate was treated dropwise during 1 h with dichlorophenylphosphine (8.0 g, 0.045 mol). The mixture was warmed to room temperature and the solution acidified with dilute ice-cold sulfuric acid. After concentration in vacuo, the residue was taken up in ether, washed with water, dried ($MgSO_4$), and concentrated to afford crude **2**. Recrystallization from ether–hexane gave **2** in 55% yield based on $PhPCl_2$: mp 102–104 °C; ^{1}H NMR δ 7.5–6.7 (m, 13 H), 4.07 (d, *J* = 1.5), 2 H, SH; ^{31}P NMR δ −19.9.

[MoCl$_4$(2-SC$_5$H$_3$NH-3-SiMe$_3$)$_2$] (3). Addition of $MoCl_5$ (0.60 g, 1.0 mmol) to **1** (0.55 g, 3.0 mmol) in CH_2Cl_2 (20 mL) resulted in a red solution. After being stirred 2 h, the solution was concentrated to ca. 4 mL and carefully layered with hexane (10 mL). After 3 days at 4 °C, dark red crystals of **3** were collected in 35% yield. Anal. Calcd for $C_{16}H_{26}N_2Si_2S_2Cl_4Mo$: C, 31.8; H, 4.31; N, 4.64. Found: C, 31.6; H, 4.03; N, 4.45. IR (KBr, cm^{-1}): 3165, 3120, 2925, 1580, 1530, 1500, 1450, 1390, 1275, 1235, 1140, 1050, 1005, 820, 670, 480, 435, 400, 295.

[MoCl$_3${2-SC$_5$H$_2$NH-3,6-(SiMe$_2$Bu^t)$_2$}$_3$] (4). To a suspension of $MoCl_4(CH_3CN)_2$ (0.300 g, 0.940 mmol) in 20 mL of CH_2Cl_2 was added HSC_5H_2N-3,6-$(SiMe_2Bu^t)_2$ (**2**) (1.00 g, 4.70 mmol), followed by NEt_3 (0.476 g, 4.70 mmol). After being stirred for 6 h at room temperature, the resultant dark red solution was concentrated to 10 mL, filtered, and treated with 30 mL of *n*-hexane. After several days, dark red crystals were isolated. Recrystallization from benzene–*n*-hexane yielded needle type crystals in 30% yield. Anal. Calcd for $C_{51}H_{99}MoN_3S_3Si_6Cl_3$: C, 50.20; H, 8.15; N, 3.44. Found: C, 50.30; H, 8.61; N, 3.28. IR (KBr, cm^{-1}): 3200, 3100, 3020, 2940, 2860, 1580, 1540, 1490, 1470, 1410, 1395, 1365, 1290, 1260, 1150, 1100, 1045, 1010, 820, 780, 675, 580, 500, 450, 420, 270. Compound **4** could be synthesized in the same way from $MoCl_5$ as starting material. Compound **4a** was synthesized in analogous fashion from $MoCl_5$ and **1**.

[Mo(2-SC$_5$H$_3$N-3-SiMe$_3$)$_4$] (5). A solution of **3** (0.60 g, 1 mmol) in acetonitrile (30 mL) was treated with tripropylamine (0.57 g, 4 mmol) in acetonitrile–CH_2Cl_2 (20 mL, 2:1). After being stirred for 2 h and concentration to 10 mL, the dark brown solution was layered with hexane. After 3 h, at 4 °C, a brown microcrystalline precipitate of **5** was collected in 25% yield. Anal. Calcd for $C_{32}H_{52}N_4Si_4S_4Mo$: C, 45.6; H, 6.18; N, 6.65. Found: C, 44.9; H, 6.01; N, 6.83. IR (KBr, cm^{-1}): 2930, 1530, 1490, 1450, 1260, 1145, 1025, 810, 670.

[MoCl$_4${2-SC$_5$H$_2$NH-3,6-(SiMe$_2$Bu^t)$_2$}$_2$]·(C$_2$H$_5$)$_2$O (6). $MoCl_5$ (0.5 g, 1.83 mmol) dissolved in CH_2Cl_2 (5 mL) was added to 2-HSC_5H_2N-3,6-$(SiMe_2Bu^t)_2$ (2.65 g, 7.80 mmol) in 20 mL of CH_2Cl_2. After being stirred for 3 days, the resultant dark green solution was concentrated to 15 mL, and 40 mL of *n*-hexane and 10 mL of diethyl ether were added. After this mixture was allowed to stand for 3 weeks at 0 °C, dark green crystals of **6** were collected in 32% yield. Anal. Calcd for $C_{38}H_{74}Cl_4MoN_4OS_2Si_4$: C, 46.2; H, 7.49; N, 2.93. Found C, 45.4; H, 7.19; N, 2.88. IR (KBr, cm^{-1}): 3180, 3120, 2930, 1580, 1530, 1500, 1460, 1400, 1360, 1280, 1250, 1230, 1140, 1090, 1040, 1000, 810, 670, 570, 490, 440, 410, 300.

(Ph$_4$P)[MoBr$_4$(2-SC$_5$H$_3$NH-3-SiMe$_3$)$_2$] (7). $[MoBr_2(CO)_4]_2$ (0.85 g, 0.025 mmol) was added to a solution of **1** (0.366 g, 2.0 mmol) in acetonitrile (10 mL) to give immediately a deep red solution. After addition of Ph_4PBr (0.41 g, 1.0 mmol) and after the mixture was stirred for ca. 24 h at room temperature, the resulting solution was evaporated to dryness, yielding a red powder. Recrystallization from CH_3OH/diethyl ether yielded dark red crystals in 20% yield. The dark red crystals were recrystallized from CH_2Cl_2/diethyl ether and washed with CH_3OH (2×). Anal. Calcd for $C_{40}H_{44}MoBr_4N_2PS_2Si_2$: C, 42.9; H, 3.93; N, 2.50. Found: C, 43.2; H, 3.85; N, 2.24. IR (KBr, cm^{-1}): 3140, 3040, 2940, 1600, 1565, 1480, 1430, 1300, 1245, 1200, 1185, 1140, 1105, 1065, 1040, 840, 750, 720, 685, 615, 525, 465, 410, 340.

[MoBr$_3$(2-SC$_5$H$_3$NH-3-SiMe$_3$)$_3$] (8). A solution of **1** (2.87 g, 15.67 mmol) in 15 mL of acetonitrile was added to $[MoBr_2(CO)_4]_2$ (1.45 g, 1.96 mmol) in 15 mL of acetonitrile. After being stirred for 24 h, the resultant dark red solution was evaporated to an oil, which was taken up in CH_2Cl_2–ether. After this oil was allowed to stand for several days at room temperature, red crystals of **8** were isolated in 25% yield. Anal. Calcd for $C_{24}H_{36}MoN_3S_3Si_3Br_3$: C, 32.7; H, 4.08; N, 4.76. Found: C, 32.5; H, 4.54; N, 4.51. IR (KBr, cm^{-1}): 3140, 3040, 2940, 1595, 1560, 1430, 1300, 1245, 1200, 1140, 1060, 1040, 1010, 840, 740, 610, 460, 405, 330.

[Mo$_2$O$_3$(2-SC$_5$H$_3$N-3-SiMe$_3$)$_4$] (9). Method 1. Addition of $MoCl_5$ (0.60 g, 1.0 mmol) to **1** (0.74 g, 4.0 mmol) in CH_2Cl_2 (20 mL) resulted in a red solution, which was concentrated to ca. 8 mL and exposed to a stream of O_2 for 5 min. After careful layering with 12 mL of diethyl ether, the solution was allowed to stand for 5 days at room temperature, and dark purple crystals of **10** were collected. Anal. Calcd for $C_{32}H_{48}Mo_2O_3S_4N_4Si_4$: C, 39.67; H, 4.95; N, 5.78. Found: C, 39.46; H, 4.98; N, 5.76. IR (KBr, cm^{-1}): 3020, 2940, 2880, 1560, 1365, 1250, 1215, 1135, 1075, 1050, 945, 840, 790, 760, 690, 670, 620, 450, 430, 340.

Method 2. A stream of O_2 was bubbled through a solution of **3** (0.30 g, 0.5 mmol) in CH_2Cl_2 (10 mL) for 10 min. After the solution was layered with diethyl ether (20 mL) and allowed to stand for 1 week at 4 °C, dark purple microcrystals of **9** were collected in 25% yield.

[MoOCl(2-SC$_5$H$_3$N-SiMe$_3$)$_2$] (10). Method 1. The Na$^+$ salt of **1** (0.793 g, 3.87 mmol) was added to $MoCl_5$ (0.21 g, 0.77 mmol) in CH_2Cl_2 (10 mL) and a small quantity of O_2 (0.25 mL) introduced by syringe through a septum seal. After being stirred for 4 h, the resultant dark red solution was evaporated to give a dark red solid, which was redissolved in ca. 10 mL of *n*-pentane. This solution was filtered and kept at −20

°C. After the solution was allowed to stand for several days, dark red crystals were isolated in 25% yield. Anal. Calcd for $C_{16}H_{24}N_2OSi_2S_2ClMo$: C, 37.5; H, 4.69; N, 5.48. Found: C, 36.9; H, 4.43; N, 5.31. IR (KBr, cm^{-1}): 3050, 2970, 1540, 1350, 1240, 1210, 1135, 1070, 1040, 840, 745, 685, 615, 470, 420, 340.

Method 2. A small portion of O_2 (0.10 mL) was added to a solution of **3** (0.20 g, 0.33 mmol) in CH_2Cl_2 (5 mL). After addition of *n*-pentane (5 mL) and after the solution was allowed to stand at −20 °C for 5 days, red microcrystals of **10** were isolated in 45% yield.

$(Ph_4)[MoOBr_3(2\text{-}SC_5H_3N\text{-}3\text{-}SiMe_3)]$ (11). Method 1. The filtrate from the crystallization of **7** was treated with wet CH_2Cl_2 (5 mL)–Et_2O (20 mL) and allowed to stand for 2 weeks. Dark green crystals of $(Ph_4P)[MoOBr_3(SC_5H_3N\text{-}3\text{-}SiMe_3)]$ (**11**) were collected in 20% yield. Anal. Calcd for $C_{32}H_{32}NOSiPSBr_3Mo$: C, 44.0; H, 3.67; N, 1.60. Found: C, 44.4; H, 3.53; N, 1.21.

Method 2. A solution of **8** (0.50 g, 0.57 mmol) in CH_2Cl_2 (20 mL) was exposed to the atmosphere for 5 min. Upon addition of diethyl ether (20 mL) and after the solution was allowed to stand for 5 days, dark green microcrystals of **11** were isolated in low yield (<10%).

$[MoCl_2(2\text{-}SC_5H_3N\text{-}3\text{-}SiMe_3)_2(NNMePh)]$ (12). Method 1. A solution of $[MoCl_4(NNMePh)]$ (0.18 g, 0.5 mmol) in methanol (5 mL) was added to a methanol solution (10 mL) of **1** (0.18 g, 1.0 mmol). After being stirred at room temperature for 60 h, the resultant red solution was concentrated to 8 mL and diethyl ether (10 mL) was added. Slow evaporation under dinitrogen gave blocky red crystals of $[MoCl_2(SC_5H_3N\text{-}3\text{-}SiMe_3)_2(NNMePh)]$ $(C_2H_5)_2O$ in 25% yield. Anal. Calcd for $C_{27}H_{42}Cl_2MoN_4OS_2Si_2$: C, 44.7; H, 5.79; N, 7.73. Found: C, 44.3; H, 5.63; N, 7.51. IR (KBr, cm^{-1}): 2920, 1560, 1480, 1445, 1370, 1250, 1215, 1150, 1130, 1080, 840, 800, 750, 645, 600, 450, 340.

Method 2. A solution of **3** (0.60 g, 1 mmol) in acetonitrile (30 mL) was treated with methylphenylhydrazine (0.12 g, 1 mmol). After the mixture was stirred for 2 h and concentrated to 8 mL, diethyl ether (20 mL) was added, resulting in the formation of a green precipitate of **12** in 20% yield.

$[Mo(2\text{-}SC_5H_3N\text{-}3\text{-}SiMe_3)_2(NNMePh)_2]$ (13). Method 1. A solution $H_2NNMePh$ (0.48 g, 4 mmol) in rigorously dry methanol (2 mL) was added slowly to a stirred solution of **3** (0.6 g, 1 mmol) in methanol (20 mL) at room temperature. After 24 h, 20 mL of diethyl ether was added to the orange solution. Upon slow evaporation under a gentle stream of argon, orange-yellow crystals of **13** were isolated in 30% yield. Anal. Calcd for $C_{30}H_{40}MoN_6S_2Si_2$: C, 51.4; H, 5.72; N, 12.01. Found: C, 51.1; H, 5.63; N, 12.2. IR (KBr, cm^{-1}): 3030, 2960, 2900, 1600, 1570, 1490, 1470, 1370, 1350, 1320, 1310, 1270, 1250, 1220, 1120, 1060, 1030, 840, 800, 755, 690, 625, 585, 540, 510, 460, 400, 350.

Method 2. A solution of **7** (0.43 g, 0.5 mmol) in CH_2Cl_2 (25 mL) was treated with $H_2NNMePh$ (0.24 g, 2 mmol). After the usual workup, yellow microcrystals of **13** were isolated in 20% yield.

$[Cl_3Mo(\mu\text{-}Cl)(\mu\text{-}2\text{-}SC_5H_3NH\text{-}3\text{-}SiMe_3)_2MoCl_2(2\text{-}SC_5H_3NH\text{-}3\text{-}SiMe_3)]\cdot 2CH_3CN$ (14). Method 1. $[MoCl_4(2\text{-}SC_5H_3NH\text{-}3\text{-}SiMe_3)_2]$ (3) (0.9 g, 1.45 mmol) dissolved in CH_2Cl_2 (10 mL) was treated with hydrazine (0.05 g, 1.4 mmol). After 20 h of stirring at room temperature, the dark red solution was concentrated to 5 mL, filtered, and carefully layered with 10 mL of diethyl ether. The resultant dark red powder was recrystallized from CH_3CN–diethyl ether to give lustrous red crystals in 20% yield.

Method 2. To $MoCl_5$ (1.50 g, 5.49 mmol) in CH_2Cl_2 (20 mL) was added diphenylacetylene (1.54 g, 8.67 mmol). After the mixture was stirred for 20 h, **1** (1.0 g, 5.5 mmol) was added to the resulting dark green-brown solution. After a further 20 h of stirring at room temperature, the solution was concentrated to 10 mL, filtered, and layered with diethyl ether (30 mL). After 5 days a dark red powder was isolated. Recrystallization from CH_3CN–diethyl ether yielded well-formed crystals in 30% yield. Anal. Calcd for $C_{24}H_{39}N_3Si_3S_3Cl_6Mo_2$: C, 30.2; H, 4.12; N, 4.40. Found: C, 29.9; H, 4.22; N, 4.72. IR (KBr, cm^{-1}): 3050, 2945, 1565, 1490, 1430, 1300, 1245, 1210, 1120, 1050, 830, 730, 620, 415, 270.

$[Cl_3Mo(\mu\text{-}Cl)\{\mu\text{-}2\text{-}SC_5H_2NH\text{-}3,6\text{-}(SiMe_2Bu^t)_2\}_2MoCl_2\{2\text{-}SC_5H_2NH\text{-}3,6\text{-}(SiMe_2Bu^t)_2\}]$ (15). To a suspension of **6** (2.0 g, 2.18 mmol) in 15 mL of diethyl ether, anhydrous hydrazine (0.280 g, 8.73 mmol) was added dropwise over 0.5 h. A brown solid was produced immediately. After the mixture was stirred for 24 h, the brown solid was collected by filtration and washed with diethyl ether. The solid was redissolved in dichloromethane (10 mL) and the solution filtered. The filtrate was slowly diluted with methanol (5 mL) and diethyl ether (20 mL). After ca. 3 weeks, dark red crystals were isolated in 40% yield. Anal. Calcd for $C_{51}H_{99}N_3Si_6S_3Cl_6Mo_2$: C, 43.03; H, 7.01; N, 2.95. Found: C, 43.44; H, 7.45; N, 3.08. IR (KBr, cm^{-1}) 3230, 3160, 3070, 2950, 2930, 2860, 1580, 1550, 1470, 1405, 1360, 1285, 1260, 1230, 1145, 1100, 1040, 1010, 820, 780, 680, 580, 495, 450, 410, 290.

$[Mo(C_6H_4O_2)\{2\text{-}SC_5H_2N\text{-}3,6\text{-}(SiMe_2Bu^t)_2\}_2]$ (16). A solution of **6** (0.8 g, 0.8 mmol) in CH_2Cl_2 (30 mL) was treated with catechol (0.11 g, 1 mmol). After this mixture was heated under reflux for 1 h and concentrated to 10 mL, the resultant dark brown solution was layered with hexane (20 mL) and allowed to stand for 3 weeks. Dark green-brown crystals of **16** were collected in 15% yield. Anal. Calcd for $C_{40}H_{68}N_2O_2Si_4S_2Mo$: C, 48.8; H, 6.91; N, 2.84. Found: C, 48.4; H, 6.43; N, 2.72.

Chart II. Organosilylated Pyridine-2-thiol Ligands **1b**, **1d**, **1e**, and **1f**

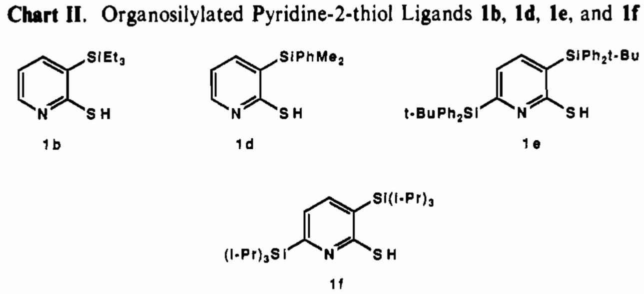

$[Mo(NNMePh)(SC_6H_4PPhC_6H_4S)_2]$ (17). A solution of $[MoCl_4(NNMePh)]$ (0.36 g, 1.0 mmol) in methanol (10 mL) was added to a methanol solution (10 mL) of $PhP(C_6H_4SH)_2$ (0.65 g, 2.0 mmol). After being stirred overnight, the solution was concentrated to 8 mL and layered with THF (15 mL). Dark green crystals of **17** were collected in 40% yield. Anal. Calcd for $C_{43}H_{34}N_2P_2S_4Mo$: C, 59.7; H, 3.94; N, 3.24. Found: C, 59.4; M, 3.86; N, 3.16. IR (KBr, cm^{-1}): 3245, 2860, 1565, 1470, 1435, 1375, 1260, 1100, 1035, 1010, 800, 740, 690, 525.

X-ray Crystal Structure Determinations. Crystal data are presented in Table I, and selected bond distances and angles are listed in Tables II–XIII. Full details of the data collection methods and refinement procedures are given in the supplementary materials and in ref 50. Tables of atomic positional parameters have been deposited as supplementary materials in the interest of conciseness. ORTEP plots of all structures, showing the full atomic labeling schemes, are also to be found in the supplementary material.

In all cases, data were collected on a Nicolet R3m/V diffractometer at −40 °C. The complexes proved invariably oxygen- and moisture-sensitive requiring careful mounting under argon and rapid transfer to the cold nitrogen stream. Crystals of the majority of the complexes of this study decompose over a period of several days at room temperature, requiring storage at −20 °C, whereupon the materials are indefinitely stable.

Solution and refinement of the structures were carried out using SHELXTL programs provided by Siemens Corp. Neutral-atom scattering factors were used throughout, and no extinction corrections were included in the refinements. Structures were solved by using Patterson methods, empirical absorption corrections were applied in several instances, and all non-hydrogen atoms were refined anisotropically. Calculated hydrogen atom positions were introduced in the final refinements.

Results and Discussion

Ligand Synthesis. Ligand synthesis was accomplished exploiting the utility of the mercapto group in directing ortho-lithiations in heterocyclic aromatic substrates. The sterically hindered pyridine-2-thiol ligands of this study are illustrated in Chart II. When THF was used as solvent and lithium diisopropylamide (LDA) was used as base, a slow deprotonation of the 3-position of pyridine-2-thiol occurred. After 8 h of stirring in THF at room temperature, a mixture of LDA, pyridine-2-thiol, and chlorotrimethylsilane gave a 55% yield of 3-(trimethylsilyl)pyridine-2-thiol (**1a**).

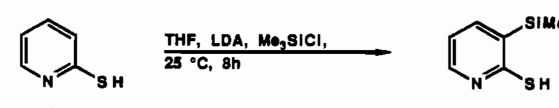

A similar reaction affords the previously unknown compounds 3-(triethylsilyl)pyridine-2-thiol (**1b**) and 3-(dimethylphenylsilyl)pyridine-2-thiol (**1d**) in 45% and 36% yields, respectively. Surprisingly, when more hindered chlorosilanes such as *tert*-butylchlorodimethylsilane, chlorotriisopropylsilane, and *tert*-butylchlorodiphenylsilane were used, the previously unknown 3,6-bis(*tert*-butyldimethylsilyl)pyridine-2-thiol (**1c**), 3,6-bis(*tert*-butyldiphenylsilyl)pyridine-2-thiol (**1e**), and 3,6-bis(triisopropyl-

(50) Nicholson, T.; Zubieta, J. *Inorg. Chem.* **1987**, *26*, 2094.

Table I. X-ray Data for the Structural Determinations of $[MoCl_3\{2\text{-}SC_5H_2NH\text{-}3,6\text{-}(SiMe_2Bu^t)_2\}_3]$ (**4**), $[MoCl_4\{2\text{-}SC_5H_2NH\text{-}3,6\text{-}(SiMe_2Bu^t)_2\}_2]\cdot(C_2H_5)_2O$ (**6**), $(Ph_4P)[MoBr_4(2\text{-}SC_5H_3NH\text{-}3\text{-}SiMe_3)_2]$ (**7**), $[MoBr_3(2\text{-}SC_5H_3NH\text{-}3\text{-}SiMe_3)_3]$ (**8**), $[Mo_2O_3(2\text{-}SC_5H_3N\text{-}3\text{-}SiMe_3)_4]$ (**9**), $[MoOCl(2\text{-}SC_5H_3N\text{-}3\text{-}SiMe_3)_2]$ (**10**), $(Ph_4P)[MoOBr_3(2\text{-}SC_5H_3N\text{-}3\text{-}SiMe_3)]$ (**11**), $[MoCl_2(2\text{-}SC_5H_3N\text{-}3\text{-}SiMe_3)_2(NNMePh)]$ (**12**), $[Mo(2\text{-}SC_5H_3N\text{-}3\text{-}SiMe_3)_2(NNMePh)_2]$ (**13**), $[Cl_3Mo(\mu\text{-}Cl)(\mu\text{-}2\text{-}SC_5H_3NH\text{-}3\text{-}SiMe_3)_2MoCl_2(2\text{-}SC_5H_3NH\text{-}3\text{-}SiMe_3)]\cdot 2CH_3Cl$ (**14**), $[Cl_3Mo(\mu\text{-}Cl)\{\mu\text{-}2\text{-}SC_5H_2NH\text{-}3,6\text{-}(SiMe_2Bu^t)_2\}_2MoCl_2\{2\text{-}SC_5H_2NH\text{-}3,6\text{-}(SiMe_2Bu^t)_2\}]$ (**15**), and $[Mo(NNMePh)(SC_6H_4PPhC_6H_4S)_2]$ (**17**)

	4	6	7	8	9	10	11	12	13	14	15	17
fw	1219	987	1119	881	968	512	873	725	700	954	1422	864
a, Å	17.644 (5)	16.245 (5)	10.689 (1)	33.376 (6)	11.719 (4)	12.858 (3)	19.806 (4)	10.727 (3)	22.833 (5)	10.605 (3)	15.338 (4)	13.466 (2)
b, Å	17.067 (5)	13.531 (4)	14.511 (3)	18.751 (4)	14.258 (7)	13.655 (3)	12.271 (3)	16.428 (5)	10.731 (2)	13.277 (4)	30.447 (8)	15.023 (2)
c, Å	25.798 (5)	23.739 (7)	16.713 (3)	11.980 (4)	14.081 (3)	13.290 (3)	32.749 (5)	22.800 (6)	14.645 (4)	16.969 (5)	33.913 (8)	21.565 (3)
α, deg	90.00	90.00	104.15 (1)	90.00	90.00	90.00	90.00	90.00	90.00	79.82 (1)	90.00	90.00
β, deg	99.17 (1)	90.00	103.58 (1)	90.00	99.91 (2)	96.67 (2)	96.57 (1)	97.67 (2)	102.25 (1)	84.19 (2)	90.00	100.05 (1)
γ, deg	90.00	90.00	95.46 (1)	90.00	90.00	90.00	90.00	90.00	90.00	71.51 (1)	90.00	90.00
V, Å^3	7669.8 (11)	5218.4 (12)	2411.6 (8)	7494.6 (13)	2317.8 (11)	2317.7 (12)	7907.4 (12)	3981 (21)	3506.9 (21)	2228.0 (11)	15838.2 (27)	4296.9 (12)
Z	4	4	2	8	2	4	8	4	4	2	8	4
space group	$P2_1/n$	*Pcan*	$P\bar{1}$	*Pbca*	$P2_1/c$	$P2_1/c$	$C2/c$	$P2_1/c$	C_2/c	$P\bar{1}$	*Pbca*	$P2_1/n$
D_{calc}, g cm^{-3}	1.06	1.26	1.54	1.56	1.39	1.47	1.46	1.21	1.33	1.54	1.19	1.34
μ(Mo Kα), cm^{-1}	44.7	60.5	36.8	37.8	38.0	39.5	34.8	57.9	53.3	30.6	45.7	37.2
no. of reflcns	2472	1533	3510	2864	1598	1843	2440	2299	2402	2249	5163	4339
R	0.089	0.073	0.053	0.032	0.032	0.086	0.083	0.077	0.051	0.053	0.059	0.038
R_w	0.091	0.076	0.058	0.031	0.035	0.089	0.092	0.075	0.059	0.052	0.054	0.042
goodness of fit	1.85	1.61	1.33	1.01	1.04	2.17	2.17	1.62	1.51	1.25	1.91	1.33

silyl)pyridine-2-thiol (**1f**) were obtained in 60%, 40%, and 30% yields, respectively. The more hindered chlorosilanes apparently substitute twice in the 3- and 6-positions while the less hindered chlorosilanes stop after one substitution in the 3-position.

When 2-pyridinethiol (**1**) is reacted with limiting LDA and a hindered chlorosilane such as *tert*-butylchlorodimethylsilane, then the 6-substituted product is obtained. Thus, the reaction of **1** with 2.5 equiv of LDA and *tert*-butylchlorodimethylsilane gives a 60% yield of an approximately 1:1 mixture of **1c** and 6-*tert*-butyldimethylsilylpyridine-2-thiol (**1g**). A reduction in the amount of

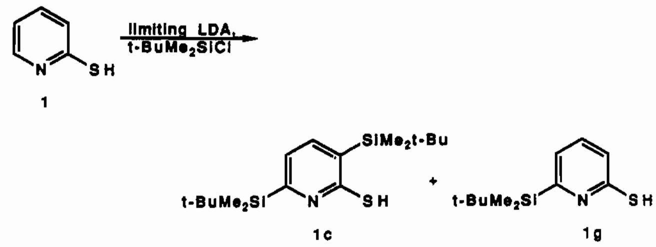

LDA to below 2.5 equiv resulted in a loss of yield without a concurrent increase in the purity of the product. The lithiation of the 6-position in compound **1** must be competitive with lithiation of the 3-position in **1g**. It is possible to obtain pure **1c** only when excess base is used. Fortunately, compounds **1c** and **1g** are easily separable by column chromatography and this method can be used to prepare **1g** on a large scale. Under no conditions could a 3-substituted pyridine-2-thiol be isolated when a "hindered" chlorosilane was used as the electrophile. GC–MS analysis of crude reaction mixtures from the reaction of **1** with hindered chlorosilanes showed that a small amount, less than 1% relative to the major products, of the appropriate 3-substituted pyridine-2-thiol was present, but in no case could it be efficiently isolated.

When 3-(trimethylsily)-2-pyridine-2-thiol (**1a**) is treated with LDA and chlorotriethylsilane, 3-(trimethylsilyl)-6-(triethylsilyl)-2-pyridinethiol (**1h**) is isolated in 28% yield.

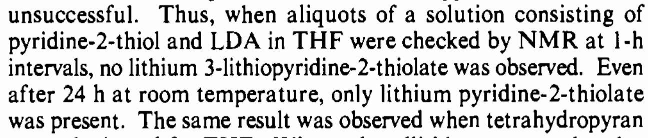

Equilibrium deprotonation of pyridine-2-thiol is useful for the preparation of 3-silylated pyridine-2-thiols and 3,6-disilylated pyridine-2-thiols. However, the current procedure lacks versatility in that the electrophilic reactant must be unreactive toward LDA. Efforts to effect the quantitative lithiation of pyridine-2-thiol were unsuccessful. Thus, when aliquots of a solution consisting of pyridine-2-thiol and LDA in THF were checked by NMR at 1-h intervals, no lithium 3-lithiopyridine-2-thiolate was observed. Even after 24 h at room temperature, only lithium pyridine-2-thiolate was present. The same result was observed when tetrahydropyran was substituted for THF. When *n*-butyllithium was used under a variety of conditions, only the 4-alkylated product was observed.

Preparation and Characterization of the Molybdenum Complexes. We have investigated the reactions of molybdenum halide precursors with these ligands and the results of these investigations are summarized in Scheme I. The reactions of **1a** with $MoCl_5$ yield a variety of products depending on the reaction conditions employed. Thus, reaction of $MoCl_5$ with the free acid form of the ligand in a 1:3 ratio in CH_2Cl_2 gave upon recrystallization brilliant red crystals of the paramagnetic complex $[MoCl_4(SNHSi)_2]$ (**3**). ($\mu = 2.49\ \mu_B$ at room temperature.) The infrared spectrum of **3** shows prominent absorptions associated with ν(Si–C) at 840 cm^{-1} and with ν(Mo–Cl) at 298 cm^{-1}. In addition, the bands observed at 3150 cm^{-1} confirm the presence of the ligand in the 1*H*-pyridine-2-thione form. The 3-(trimethylsilyl)pyridine-2-thiol serves not only as a neutral ligand but also as a reducing agent to afford the Mo(IV) complex **1a**.

In contrast, the reaction of $MoCl_5$ with excess **1a** in the presence of triethylamine results in further reduction and isolation of the brown paramagnetic Mo(III) species $[MoCl_3(SNHSi)_3]$ (**4a**),

Scheme I. Reaction Chemistry of Molybdenum Halide Precursors with the Ligands **1a** and **1c**

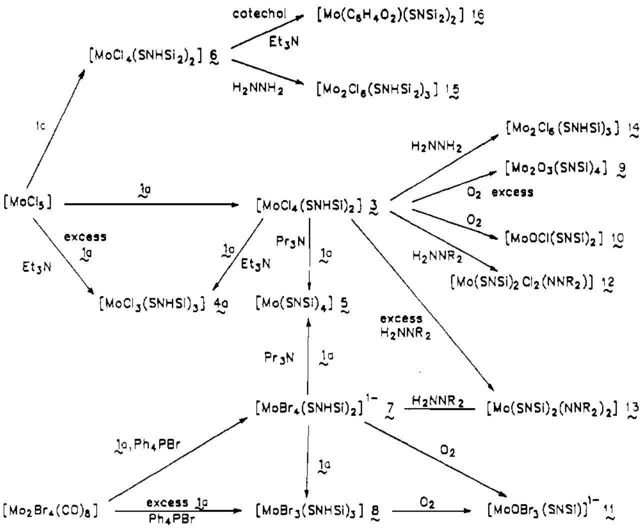

which may also be prepared by addition of **1a** to solutions of **3**. The infrared spectrum of **4a** exhibits characteristic ligand bands at 3120 and 820 cm^{-1} and a feature at 300 cm^{-1} attributed to ν(Mo–Cl). The room-temperature magnetic moment of **4a** is 3.63 μ_B.

The consequences of increased steric bulk of the ligand are apparent in the reaction of $MoCl_5$ with **1c**, which yields dark green paramagnetic crystals of $[MoCl_4(SNHSi_2)_2]$ (**6**). In contrast to the cis geometry adopted by the thione ligands of **3**, the 3,6-bis(trimethylsilyl)-1*H*-pyridine-2-thione ligands of **6** occupy trans positions, as confirmed by the X-ray studies of this work. The infrared spectrum of **6** is unexceptional for this type of complex, showing the characteristic ligand bands at 3100 and 810 cm^{-1} and a band at ca. 300 cm^{-1} associated with ν(Mo–Cl). In contrast to the behavior of **3**, addition of ligand **2** to **6** did not result in reaction to give the analogous $[MoCl_3(SNHSi_2)_3]$ species, possibly as a consequence of the increased steric demands of **1c**. Complex **4** could be isolated, however, directly from the reaction of $[MoCl_4(CH_3CN)_2]$ with excess **2**.

The chemistry of the Mo-bromide series of complexes did not entirely parallel that of the Mo–chloride series discussed above. Reactions of $MoBr_5$ with **1a** and **1c** yielded only intractable materials. However, the reaction of $[MoBr_2(CO)_4]_2$ with **1a** in a 1:4 molar ratio resulted in oxidation of the Mo(II) of the starting material to Mo(III) in $[MoBr_4(SNHSi)_2]^-$ (**7a**), which was isolated as the $(Ph_4P)^+$ salt. The paramagnetic compound is a 1:1 electrolyte (Λ_M = 57 Ω^{-1} cm mol^{-1} at 20 °C in $MeNO_2$–CH_2Cl_2). The infrared spectrum of **7** exhibits absorptions associated only with the ligands, with a prominent feature at 840 cm^{-1} characteristic of ν(Si–C) and a medium-intensity band at 3060 cm^{-1} assigned to ν(N–H) for the thione form of the ligand. The reaction of **7** with **1a** yields the Mo(III) species $[MoBr_3(SNHSi)_3]$ **8**, which is directly analogous to the chloride species **4** and exhibits a room-temperature moment of 3.69 μ_B.

The persistence of the thione form of ligands **1a** and **1c** in these complexes was unexpected. The only structurally characterized complex of molybdenum with pyridine-2-thiol, $[Mo_2O_3(C_5H_4NS)_4]$, exhibits the thiolate form of the ligand,[37] while reactions of $[MoCl_4(thf)_2]$ and $MoCl_5$ with the analogous pyrimidine-2-thiol yield only the eight-coordinate $[Mo(C_4H_3N_2S)_4]$, which also displays the ligand thiolate form.[51] In fact, reactions of pyridine-2-thiol with $MoCl_5$ or $[MoCl_4(thf)_2]$ under the conditions employed in this study yield only intractable materials. This observation confirms the utility of organosilyl substituents in preventing polymerization and in affording materials soluble in common organic solvents.

(51) Latham, I. A.; Leigh, G. J.; Pickett, C. J.; Huttner, G.; Jibrill, I.; Zubieta, J. *J. Chem. Soc., Dalton Trans.* **1986**, 1181.

Chart III. Possible Structural Types for $[Mo(2\text{-}SC_5H_3N\text{-}3\text{-}SiMe_3)_4]$ (**5**)

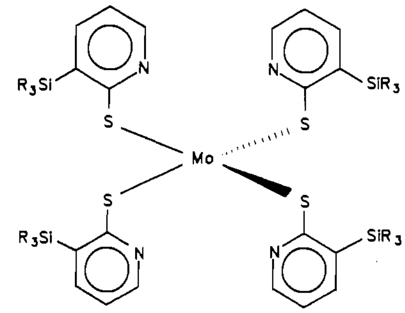

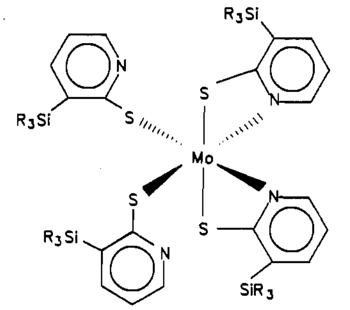

Likewise, the persistence of mixed halido–thione coordination to molybdenum centers in mononuclear cores is unusual. The structurally characterized example of mixed halido–thiolate coordination, $[MoCl_2(SC_6H_4SCH_2CH_2SC_6H_4S)]$,[52] and the chemically characterized $[MoCl(2,4,6\text{-}Pr^i_3\text{-}C_6H_2S)_4]$[9] also rely upon steric or geometric characteristics of the thiolate donors to retain halide coordination. The steric requirements of ligands of the class of which **1a** and **1c** are prototypes would preclude exclusively thiolate or thione ligation to satisfy the Mo coordination, thus necessitating halide ligation to complete the geometry. The charge requirement of the Mo center would seem to preclude isolation of the entire series of halido–thione complexes $[Mo(SNSi)_{2+n}X_{4-n}]$ (X = halide, n = 1–4).

Deprotonation of the coordinated ligand thione form may be effected, however, by titration of solutions of **3** or **7** with tetra-*n*-butylammonium hydroxide ((TBA)OH) in the presence of excess ligand **1a**, yielding in both instances the mononuclear paramagnetic species $[Mo(SNSi)_4]$ (**5**) (μ = 2.35 μ_B at room temperature). The infrared spectrum of **5** exhibits a strong absorption at 820 cm^{-1} attributed to ν(Si–C) and no observable feature in the 3000–3200-cm^{-1} region or in the 300-cm^{-1} range, confirming the displacement of both the N-bound proton and the chloride donors. Solutions of **5** proved extremely sensitive to moisture and temperature and X-ray quality crystals were not obtained. A number of possible structures may be considered for **5**. An eight-coordinate geometry similar to that reported for $[Mo(C_4H_3N_2S)_4]$ is unlikely as Mo(IV) species of this type are characteristically diamagnetic. Of the alternatives J and K illustrated in Chart III, the distorted octahedral type K would result in severe steric crowding, while structure J should allow the ligands to adopt an orientation minimizing steric interactions of the triorganosilyl groups in a manner akin to that observed for the diamagnetic distorted tetrahedral species $[Mo(2,4,6\text{-}Pr^i_3\text{-}C_6H_2S)_4]$.[9]

As anticipated, the Mo(III)- and Mo(IV)–halido–thione complexes, **5**, **4**, **7**, and **8**, are extremely oxophilic, reacting with O_2 to give Mo(V) species with compositions dependent on reaction conditions and the nature of the starting material. Thus, when a stream of O_2 is bubbled through a CH_2Cl_2 solution of **3**, a deep purple Mo(V) species with the ubiquitous $[Mo_2O_3]^{4+}$ core is

(52) Kaul, B. B.; Sellmann, D. *Z. Naturforsch.* **1983**, *38B*, 562.

isolated. The infrared spectrum of $[Mo_2O_3(SNSi)_4]$ (**9**) exhibits prominent absorptions in the 750–943-cm^{-1} region consistent with the presence of both terminal and bridging oxo groups. The absence of absorptions in the characteristic ν(N–H) region, 3000–3200 cm^{-1}, confirms the presence of the thiolate form of the ligand.

In contrast to the behavior in the presence of a large excess of O_2, a controlled introduction of O_2 into a solution of **3** yields a mononuclear Mo(V) species $[MoOCl(SNSi)_2]$ **10**. The infrared spectrum of **10** exhibits a strong feature at 945 cm^{-1} assigned to $\nu(Mo{=}O_t)$ and a medium-intensity band at 290 cm^{-1} consistent with the presence of a chloride ligand. The EPR spectrum of **10** in acetonitrile at room temperature exhibits a central line at $g = 2.001$ and hyperfine splitting of six lines arising from $I = {}^5/_2$ of ^{97}Mo and ^{95}Mo isotopes (A = 4.1 mT).

To our surprise, the reactions of **7** and **8** with O_2 did not yield the analogous $[MoOBr(SNSi)_2]$ complex but rather the anionic Mo(V) species $[MoOBr_3(SNSi)]^-$ (**11a**), isolated as the Ph_4P^+ salt. The infrared spectrum of **11** was unexceptional, with an intense band at 942 cm^{-1}, assigned to $\nu(Mo{=}O_t)$, and the ligand features at ca. 800 cm^{-1} dominating the spectrum. The room-temperature EPR spectrum taken in acetonitrile exhibits a central line at $g = 1.99$ and six-line hyperfine splitting with A = 4.3 mT.

Since the reactions of molybdenum complexes in sulfur environments with nitrogen-containing substrate molecules are of particular interest to us, the chemistry of **3**, **7**, and **8** with organohydrazine ligands was investigated. As anticipated, the halide ligands of these species are readily displaced by a variety of donors. Reaction of **3** with excess *N,N*-methylphenylhydrazine yields $[Mo(SNSi)_2(NNMePh)_2]$ (**13**) as orange diamagnetic crystals. The infrared spectrum of **13** is characterized by strong bands at 1565 and 1595 cm^{-1} assigned to ν_a(N=N) and ν_s(N=N) for the *cis*-bis(hydrazido(2–)) unit and at 750–850 cm^{-1} assigned to ν(Si—C).

The displacement of four chloride donors by two strongly p-bonding hydrazido(2–) groups requires ligation of the pyridyl nitrogen to satisfy the coordination requirements of the Mo center. In a formal sense, the Mo(IV) center of **3** undergoes oxidation to the Mo(VI) state. The *cis*-bis(hydrazido(2–))–Mo(VI) core has been identified previously for $[Mo(NNMePh)_2(S_2CNMe_2)_2]$[53] and $[Mo(NNMe_2)_2(bpy)_2]^{2+}$,[53] and detailed mechanistic studies of the degradation of coordinated organohydrazines by acid have been reported.[54] In contrast, the reaction of **3** with 1 equiv of $H_2NNMePh$ or reaction of $[MoCl_4(NNMePh)]$ with **1a** yields red diamagnetic crystals of the seven-coordinate monosubstituted species $[MoCl_2(SNSi)_2(NNMePh)]$ (**12**). The infrared spectrum of **12** reveals the presence of the coordinated hydrazido(2–) ligand (1563 cm^{-1}) and prominent features at 840 cm^{-1} and 335 cm^{-1} assigned to ν(Si–C) and ν(Mo–Cl), respectively. Since the complex is a nonelectrolyte and ligand mode E is indicated by the absence of infrared bands in the 3000-cm^{-1} region, **12** adopts the seven-coordinate geometry common to complexes of the types $[MoCl_2(S_2CNR_2)_2(NNR_2)]$[55] and $[Mo(SCH_2CH_2PPhCH_2CH_2S)_2(NNR_2)]$.[56]

Hydrazine itself acts as a reducing agent in reactions with **3**. Although reductions of Mo–thiolate species by hydrazine generally yield intractable materials, the reduction of **3** proceeds smoothly to give the binuclear Mo(III) complex $[Mo_2Cl_6(SNHSi)_3]$ (**14**). The optimal reaction conditions are 4 equiv of **3** to 1 equiv of hydrazine indicating the simple stoichiometry

$$4[MoCl_4(2\text{-}SC_5H_3NH\text{-}3\text{-}SiMe_3)_2] + H_2NNH_2 \rightarrow 2[Mo_2Cl_6(SNHSi)_3] + 4HCl + N_2 + 2HSC_5H_3N\text{-}3\text{-}SiMe_3$$

The infrared spectrum of **14** exhibits ligand features at 3050 and 830 cm^{-1} assigned to ν(N–H) and ν(Si–C), respectively, and a strong band at 270 cm^{-1}, consistent with ν(Mo–Cl). The complex is diamagnetic and a nonelectrolyte with the molecular weight consistent with a binuclear formulation, a feature confirmed by the X-ray study (vide infra). Reaction of **6** with hydrazine yields the analogous binuclear complex **15**, indicating that the augmented steric encumbrance of the ligand does not grossly influence product composition.

In general, the thione ligand form appears to be characteristic of complexes of molybdenum in the lower oxidation states, Mo(III) and Mo(IV), while those complexes that contain molybdenum centers formally in the Mo(V) and Mo(VI) oxidation states exhibit the thiolate coordination mode.

The halide ligands of **3** and **4** may also be displaced by various dianionic chelating ligands, such as catechol, to give complexes of the type $[Mo(C_6H_4O_2)(SNSi_2)_2]$ (**16**). Although the ligand **1c** most likely adopts the chelating thiolate mode in the paramagnetic mononuclear Mo(IV) species, X-ray quality crystals of **16** could not be isolated to confirm this assignment. Attempts to displace the chloride donors with monodentate pseudohalides, such as azide and thiocyanate, yield intractable materials or mixtures that decomposed during separation attempts.

Description of the Structures. The complexes of this study may be divided into four general structural types: (i) mononuclear halido–thione complexes of Mo(III) and Mo(IV), **4**, **6**, **7**, and **8**; (ii) binuclear halido–thione complexes of Mo(III), **14** and **15**; (iii) oxo–thiolato complexes of Mo(V), **9**–**11**; and (iv) hydrazido(2)–thiolate complexes of Mo(VI), **12**, **13**, and **17**.

The structures of the Mo(III) complexes of the class $[MoX_3L_3]$ (X = Cl, L = $(SNHSi_2)$ (**4**); X = Br, L = (SNHSi) (**8**)) are illustrated in Figures 1 and 2 and the relevant bonding parameters are summarized in Tables II and V. The structures consist of

Table II. Selected Bond Lengths (Å) and Angles (deg) for **4**

Mo–Cl(1)	2.438 (9)	Mo–S(1)	2.516 (9)
Mo–Cl(2)	2.442 (8)	Mo–S(2)	2.515 (9)
Mo–Cl(3)	2.454 (9)	Mo–S(3)	2.513 (9)
S(1)–C(11)	1.75 (2)	S(3)–C(31)	1.74 (2)
S(2)–C(21)	1.72 (2)		
Cl(1)–Mo–Cl(2)	91.6 (3)	Cl(1)–Mo–S(2)	173.2 (3)
Cl(1)–Mo–Cl(3)	90.9 (3)	Cl(2)–Mo–S(2)	89.6 (3)
Cl(2)–Mo–Cl(3)	92.2 (3)	Cl(3)–Mo–S(2)	95.7 (3)
Cl(1)–Mo–S(1)	92.0 (3)	Cl(1)–Mo–S(3)	91.8 (3)
Cl(2)–Mo–S(1)	90.8 (3)	Cl(2)–Mo–S(3)	175.2 (3)
Cl(3)–Mo–S(1)	175.7 (3)	Cl(3)–Mo–S(3)	91.1 (3)
S(1)–Mo–S(2)	81.3 (3)	Mo–S(1)–C(11)	116.2 (7)
S(1)–Mo–S(3)	85.6 (3)	Mo–S(2)–C(21)	115.6 (7)
S(2)–Mo–S(3)	86.6 (3)	Mo–S(3)–C(31)	117.2 (7)

Table III. Selected Bond Lengths (Å) and Angles (deg) for **6**

Mo–Cl(1)	2.404 (5)	Mo–S(1)	2.418 (5)
Mo–Cl(2)	2.388 (5)		
S(1)–C(1)	1.75		
Cl(1)–Mo–Cl(2)	90.7 (2)	Cl(2)–Mo–S(1)	91.8 (2)
Cl(1)–Mo–S(1)	88.2 (1)	Cl(1)–Mo–Cl(2a)	89.3 (2)
Mo–S(1)–C(1)	116.1 (7)		

Table IV. Selected Bond Lengths (Å) and Angles (deg) for **7**

Mo–Br(1)	2.566 (2)	Mo–Br(4)	2.611 (2)
Mo–Br(2)	2.605 (2)	Mo–S(1)	2.495 (3)
Mo–Br(3)	2.616 (2)	Mo–S(2)	2.509 (3)
S(1)–C(11)	1.71 (1)	S(2)–C(21)	1.71 (1)
Br(1)–Mo–Br(2)	175.0 (1)	Br(1)–Mo–S(2)	87.3 (1)
Br(1)–Mo–Br(3)	90.4 (1)	Br(2)–Mo–S(1)	86.6 (1)
Br(1)–Mo–Br(4)	92.3 (1)	Br(2)–Mo–S(2)	88.4 (1)
Br(2)–Mo–Br(3)	92.4 (1)	Br(3)–Mo–S(1)	177.5 (1)
Br(2)–Mo–Br(4)	91.9 (1)	Br(3)–Mo–S(2)	94.8 (1)
Br(3)–Mo–Br(4)	88.8 (1)	Br(4)–Mo–S(1)	93.5 (1)
Br(1)–Mo–S(1)	90.4 (1)	Br(4)–Mo–S(2)	82.9 (1)
Mo–S(1)–C(11)	115.5 (4)	Mo–S(2)–C(21)	114.3 (5)

(53) Chatt, J.; Crichton, B. A. L.; Dilworth, J. R.; Dahlstrom, P.; Gutkosha, R.; Zubieta, J. A. *Inorg. Chem.* **1982**, *21*, 2383.
(54) Dilworth, J. R.; Henderson, R. A.; Dahlstrom, P.; Nicholson, T.; Zubieta, J. A. *J. Chem. Soc., Dalton Trans.* **1987**, 529.
(55) Chatt, J.; Crichton, B. A. L.; Dilworth, J. R.; Dahlstrom, P.; Zubieta, J. A. *J. Chem. Soc., Dalton Trans.* **1982**, 1041.
(56) Dilworth, J. R.; Hutchinson, J.; Throop, L.; Zubieta, J. *Inorg. Chim. Acta* **1983**, *79*, 208.

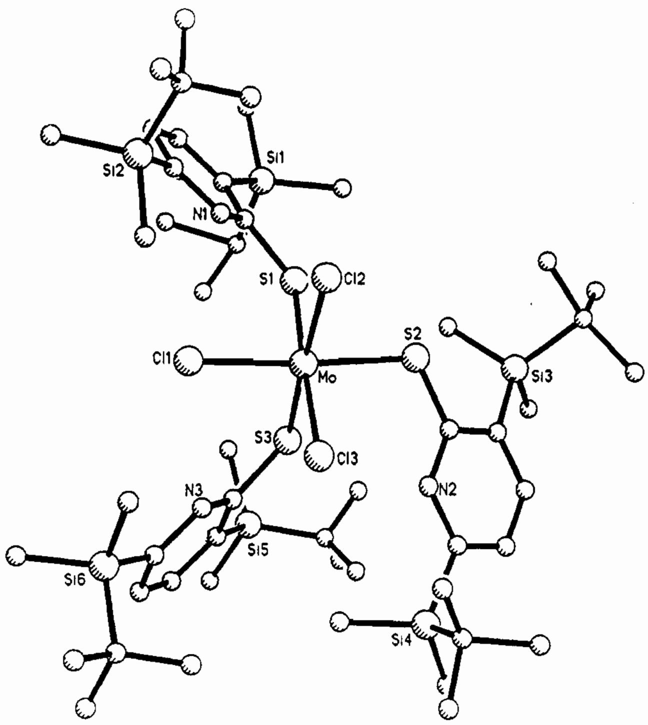

Figure 1. View of the structure of $[MoCl_3\{2\text{-}SC_5H_2NH\text{-}3,6\text{-}(SiMe_2Bu^t)_2\}_3]$ (**4**).

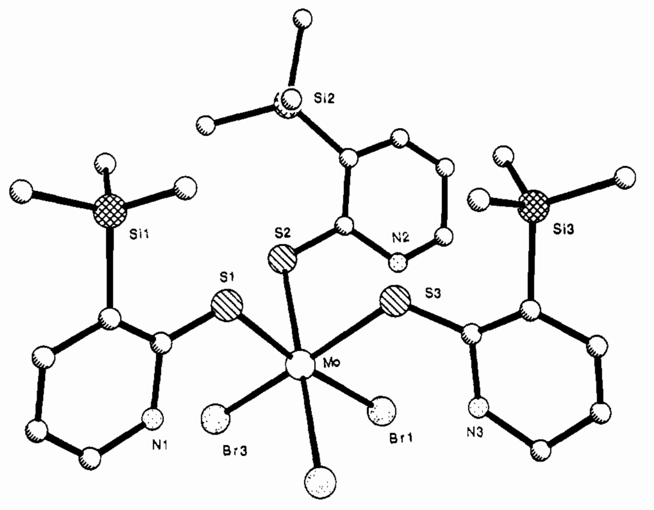

Figure 2. Perspective view of the structure of $[MoBr_3(2\text{-}SC_5H_3NH\text{-}3\text{-}SiMe_3)_3]$ (**8**).

Table V. Selected Bond Lengths (Å) and Angles (deg) for **8**

Mo–Br(1)	2.619 (1)	Mo–S(1)	2.502 (2)
Mo–Br(2)	2.600 (1)	Mo–S(2)	2.487 (2)
Mo–Br(3)	2.590 (1)	Mo–S(3)	2.492 (2)
S(1)–C(11)	1.714 (9)	S(3)–C(31)	1.703 (10)
S(2)–C(21)	1.714 (8)		
Br(1)–Mo–Br(2)	90.4 (1)	Br(3)–Mo–S(2)	89.5 (1)
Br(1)–Mo–Br(3)	90.3 (1)	Br(1)–Mo–S(3)	93.4 (1)
Br(2)–Mo–Br(3)	89.6 (1)	Br(2)–Mo–S(3)	94.3 (1)
Br(1)–Mo–S(1)	173.8 (1)	Br(3)–Mo–S(3)	174.6 (1)
Br(2)–Mo–S(1)	93.6 (1)	S(1)–Mo–S(2)	79.3 (1)
Br(3)–Mo–S(1)	94.4 (1)	S(1)–Mo–S(3)	81.7 (1)
Br(1)–Mo–S(2)	96.8 (1)	S(2)–Mo–S(3)	86.2 (1)
Br(2)–Mo–S(2)	172.8 (1)		
Mo–S(1)–C(11)	118.2 (3)	Mo–S(3)–C(31)	117.1 (3)
Mo–S(2)–C(21)	115.6 (3)		

mononuclear Mo(III) centers in a distorted octahedral environment of three halide and three thione sulfur donors. In both cases, the facial ligand geometry has been adopted. This observation

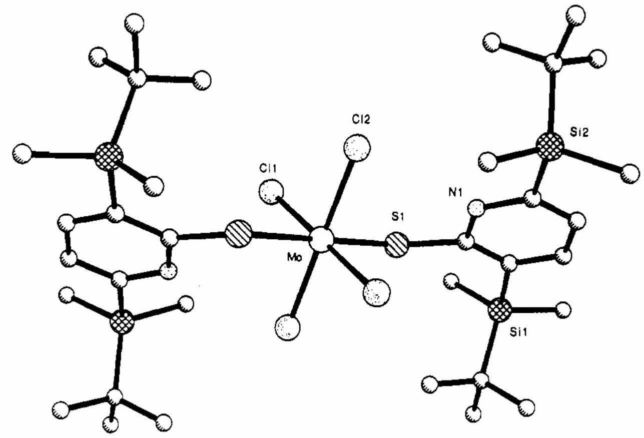

Figure 3. Structure of $[MoCl_4\{2\text{-}SC_5H_2NH\text{-}3,6\text{-}(SiMe_2Bu^t)_2\}_2]$ (**6**), omitting the $(C_2H_5)_2O$ molecule of crystallization.

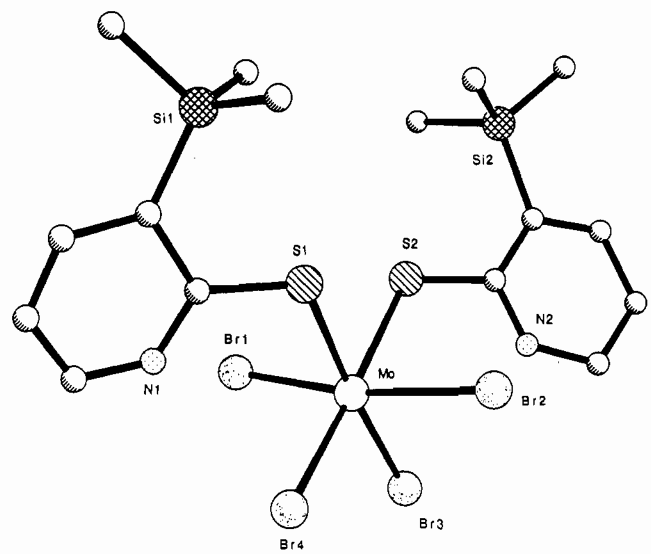

Figure 4. Structure of the molecular anion $[MoBr_4(2\text{-}SC_5H_3NH\text{-}3\text{-}SiMe_3)_2]^-$ of **7**.

is somewhat unusual since the complexes of the $[MoX_3L_3]$ class generally adopt the meridional arrangement,[57] except in cases where a facially directing ligand, such as 1,4,7-triazacyclononane[58] or tris(pyrazoyl)borate,[59] is present. The facial ligand geometry adopted by **4** and **8** may reflect the weak π-donor nature of the thione ligands,[60] whose π-overlap with the Mo t_{2g} orbitals is maximized in this geometry. On the other hand, the steric constraints imposed by the $(SNHSi_2)$ ligand might be expected to favor the less sterically encumbered meridional form, particularly since the Mo(IV) species $[MoCl_4\ (SNHSi_2)]$ (**6**), shown in Figure 3, adopts the trans configuration, rather than the cis geometry generally favored by sulfur donor types. It appears that an interplay of steric and electronic features of the structures may determine the ligand geometry to be adopted. In the case of the Mo(III) d^3 complexes, maximizing the π-interaction appears to provide the driving force for the facial ligand arrangement, a geometry that may be accommodated in **8** by orienting two of the ligand ring places approximately perpendicular to the third. In contrast, the Mo(IV) d^2 geometries seem to reflect both steric and electronic factors since the trans geometry of **6** must reflect steric influence and the localization of Mo nonbonding electrons in the d_{xy} orbital in the plane perpendicular to the S–Mo–S axis of the structure.

(57) Brencic, J. V. *Z. Anorg. Allg. Chem.* **1974**, *403*, 218.
(58) Backes-Dahmann; Hermann, W.; Weighardt, K.; Weiss, J. *Inorg. Chem.* **1985**, *24*, 485.
(59) Millar, M.; Lincoln, S.; Koch, S. A. *J. Am. Chem. Soc.* **1982**, *104*, 288.
(60) Blower, P. J.; Dilworth, J. R.; Hutchinson, J. P.; Zubieta, J. A. *J. Chem. Soc. Dalton Trans.* **1985**, 1533.

Table VI. Selected Bond Lengths (Å) and Angles (deg) for **9**

Mo(1)-S(1)	2.490 (2)	Mo(1)-O(2)	1.680 (4)
Mo(1)-S(2)	2.452 (2)	Mo(1)-N(1)	2.328 (5)
Mo(1)-O(1)	1.863 (1)	Mo(1)-N(2)	2.199 (5)
S(1)-C(1)	1.755 (6)	S(2)-C(2)	1.769 (6)
S(1)-Mo(1)-S(2)	148.6 (1)	S(2)-Mo(1)-N(2)	88.5 (1)
S(1)-Mo(1)-O(1)	98.7 (1)	O(1)-Mo(2)-O(2)	105.0 (2)
S(1)-Mo(1)-O(2)	95.1 (2)	O(1)-Mo(2)-N(1)	86.3 (1)
S(1)-Mo(1)-N(1)	64.1 (1)	O(1)-Mo(2)-N(2)	153.9 (1)
S(1)-Mo(1)-N(2)	91.0 (2)	O(2)-Mo(2)-N(1)	158.0 (2)
S(2)-Mo(1)-O(1)	94.4 (1)	O(2)-Mo(2)-N(2)	98.1 (2)
S(2)-Mo(1)-O(2)	108.9 (2)	N(1)-Mo(2)-N(2)	76.2 (2)
S(2)-Mo(1)-N(1)	64.1 (1)		
Mo(1)-S(1)-C(1)	84.6 (2)	Mo(1)-S(2)-C(11)	82.5 (2)

Table VII. Selected Bond Lengths (Å) and Angles (deg) for **10**

Mo-Cl	2.267 (6)	Mo-S(2)	2.456 (4)
Mo-O	1.782 (12)	Mo-N(1)	2.18 (1)
Mo-S(1)	2.429 (4)	Mo-N(2)	2.30 (1)
S(1)-C(11)	1.76 (2)	S(2)-C(21)	1.76 (2)
Cl-Mo-S(1)	91.2 (2)	S(1)-Mo-N(2)	89.3 (3)
Cl-Mo-S(2)	98.3 (2)	S(2)-Mo-O	95.5 (3)
Cl-Mo-O	104.6 (4)	S(2)-Mo-N(1)	95.7 (3)
Cl-Mo-N(1)	153.2 (4)	S(2)-Mo-N(2)	64.4 (3)
Cl-Mo-N(2)	90.8 (3)	O-Mo-N(1)	96.6 (5)
S(1)-Mo-S(2)	152.1 (2)	O-Mo-N(2)	156.6 (4)
S(1)-Mo-O	107.5 (3)	N(1)-Mo-N(2)	74.8 (5)
S(1)-Mo-N(1)	66.6 (3)		
Mo-S(1)-C(11)	82.2 (5)	Mo-S(2)-C(21)	84.8 (5)

Table VIII. Selected Bond Lengths (Å) and Angles (deg) for **11**

Mo-Br(1)	2.517 (3)	Mo-S(1)	2.467 (7)
Mo-Br(2)	2.525 (3)	Mo-N(1)	2.28 (2)
Mo-Br(3)	2.509 (4)	Mo-O	1.64 (2)
S(1)-C(1)	1.70 (2)		
Br(1)-Mo-Br(2)	166.3 (1)	Br(2)-Mo-S(3)	153.8 (2)
Br(1)-Mo-Br(3)	87.6 (1)	Br(1)-Mo-O	97.3 (5)
Br(2)-Mo-Br(3)	87.6 (1)	Br(2)-Mo-O	96.4 (5)
Br(1)-Mo-S(1)	91.2 (2)	Br(3)-Mo-O	111.0 (6)
Br(2)-Mo-S(2)	87.4 (2)		
S(1)-Mo-O	95.1 (6)	S(1)-Mo-N(1)	64.0 (5)
Br(1)-Mo-N(1)	84.6 (4)	O-Mo-N(1)	159.0 (7)
Br(2)-Mo-N(1)	82.5 (4)	Mo-S(1)-C(1)	84.7 (8)
Br(3)-Mo-N(1)	89.9 (4)		

The structures of the $[MoX_4L_2]^n$, class (X = Cl, L = (SNHSi$_2$), $n = 0$ (**6**); and X = Br, L = (SNHSi), $n = -1$ (**7**)) are illustrated in Figures 3 and 4. The structure of the Mo(III) species **7** is unexceptional, displaying distorted octahedral geometry with a cis configuration of the thione ligands. In both a formal and a synthetic sense, complex **8** is related to **7** by substitution of a neutral thione ligand for a chloride donor. The cis arrangement of thione donors in **7** reflects the tendency of weak p-donor ligands to maximize overlap with the metal t_{2g} orbitals. In contrast, the Mo(IV) complex **6** adopts the trans thione geometry, as discussed above.

Although a number of neutral complexes of the type $[MoX_4L_2]$ have been described, the neutral ligands L are generally N or P donors[61-66] and are rarely O donors.[62,67] Furthermore, complexes of this type or of the $[MoX_3L_3]$ class cannot be isolated by using the unsubstituted pyridine-2-thiol, confirming the special stability often afforded by sterically encumbering substituents.

(61) Allen, E. A.; Brisdon, B. J.; Fowles, G. W. A. *J. Chem. Soc.* **1964**, 4531.
(62) Allen, E. A.; Freeman, K.; Fowles, G. W. A. *J. Chem. Soc.* **1965**, 1636.
(63) Carmichael, W. M.; Edwards, D. A. *J. Inorg. Nucl. Chem.* **1972**, *34*, 1181.
(64) Miniscloux, C.; Martino, G.; Sajus, L. *Bull. Soc. Chim. Fr.* **1973**, 2179.
(65) Moss, J. R.; Shaw, B. L. *J. Chem. Soc. A* **1970**, 595.
(66) Butcher, A. V.; Chatt, J. *J. Chem. Soc. A* **1970**, 2652.
(67) Varadi, Z. B.; Nieuwpoort, A. *Inorg. Nucl. Chem. Lett.* **1974**, *10*, 801.

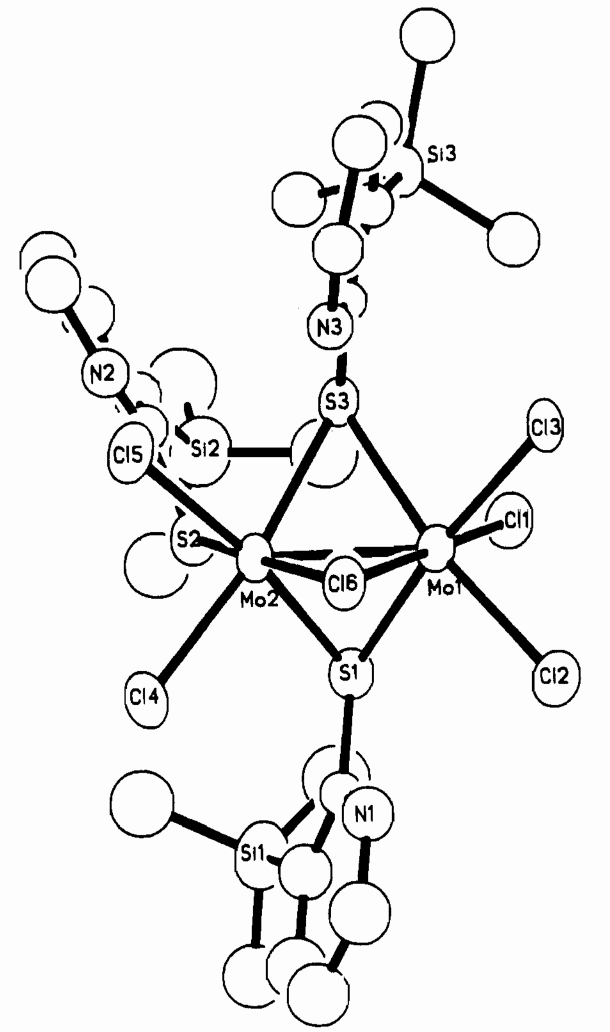

Figure 5. Perspective view of the structure of $[Mo_2Cl_6(2\text{-}SC_5H_3NH\text{-}3\text{-}SiMe_3)_3]$ (**14**).

Table IX. Selected Bond Lengths (Å) and Angles (deg) for **12**

Mo-Cl(1)	2.416 (4)	Mo-N(1)	2.21 (1)
Mo-Cl(2)	2.451 (4)	Mo-N(2)	2.21 (1)
Mo-S(1)	2.496 (5)	Mo-N(3)	1.75 (1)
Mo-S(2)	2.508 (4)		
N(3)-N(4)	1.30 (2)	S(2)-C(21)	1.72 (2)
S(1)-C(11)	1.76 (2)		
Cl(1)-Mo-Cl(2)	84.1 (2)	Cl(2)-Mo-N(1)	88.6 (4)
Cl(1)-Mo-S(1)	144.6 (2)	Cl(2)-Mo-N(2)	88.2 (3)
Cl(1)-Mo-S(2)	69.0 (2)	Cl(2)-Mo-N(3)	176.0 (4)
Cl(1)-Mo-N(1)	80.9 (4)	S(1)-Mo-S(2)	69.0 (1)
Cl(1)-Mo-N(2)	81.8 (3)	S(1)-Mo-N(1)	64.3 (4)
Cl(1)-Mo-N(3)	92.0 (4)	S(1)-Mo-N(2)	132.7 (3)
Cl(2)-Mo-S(1)	89.0 (2)	S(1)-Mo-N(3)	94.8 (4)
Cl(2)-Mo-S(2)	87.3 (2)		
N(1)-Mo-N(2)	162.6 (5)	Mo-N(3)-N(4)	171.3 (11)
N(1)-Mo-N(3)	91.9 (5)	Mo-S(1)-C(11)	83.4 (6)
N(2)-Mo-N(3)	90.2 (5)	Mo-S(2)-C(21)	84.3 (6)

Table X. Selected Bond Lengths (Å) and Angles (deg) for **13**

Mo-S(1)	2.496 (1)	S(1)-C(1)	1.759 (5)
Mo-N(1)	2.276 (4)	N(2)-N(3)	1.310 (5)
Mo-N(2)	1.782 (4)		
S(1)-Mo-N(1)	64.2 (1)	Mo-S(1)-C(1)	83.3 (2)
S(1)-Mo-N(2)	99.6 (1)	Mo-N(2)-N(3)	172.3 (3)
N(1)-Mo-N(2)	92.1 (2)		

A comparison of the average Mo-S and Mo-Cl distances for **4** and **6**, 2.515 (18) vs 2.418 (5) Å and 2.445 (18) vs 2.396 (18) Å, respectively, illustrates the anticipated reduction in both lengths

Table XI. Selected Bond Lengths (Å) and Angles (deg) for **14**

Mo(1)-Mo(2)	2.445 (2)	Mo(2)-S(1)	2.447 (5)
Mo(1)-S(1)	2.467 (5)	Mo(2)-S(2)	2.473 (6)
Mo(1)-S(3)	2.465 (4)	Mo(2)-S(3)	2.471 (5)
Mo(1)-Cl(1)	2.390 (6)	Mo(2)-Cl(4)	2.434 (5)
Mo(1)-Cl(2)	2.449 (4)	Mo(2)-Cl(5)	2.455 (5)
Mo(1)-Cl(3)	2.429 (4)	Mo(2)-Cl(6)	2.529 (5)
Mo(1)-Cl(6)	2.537 (6)	S(1)-C(11)	1.76 (2)
		S(2)-C(21)	1.74 (2)
		S(3)-C(31)	1.75 (2)
S(1)-Mo(1)-S(3)	99.6 (1)	S(1)-Mo(2)-S(2)	77.4 (2)
S(1)-Mo(1)-Cl(1)	81.7 (2)	S(2)-Mo(2)-S(3)	80.7 (2)
S(3)-Mo(1)-Cl(1)	82.7 (2)	S(1)-Mo(2)-Cl(4)	85.5 (2)
S(1)-Mo(1)-Cl(2)	88.7 (1)	S(2)-Mo(2)-Cl(4)	93.9 (2)
S(3)-Mo(1)-Cl(2)	171.3 (2)	S(3)-Mo(2)-Cl(4)	171.2 (1)
Cl(1)-Mo(1)-Cl(2)	94.6 (2)	S(1)-Mo(2)-Cl(5)	170.7 (2)
S(1)-Mo(1)-Cl(3)	172.5 (2)	S(2)-Mo(2)-Cl(5)	99.2 (2)
S(3)-Mo(1)-Cl(3)	95.5 (1)	S(3)-Mo(2)-Cl(5)	88.0 (2)
Cl(1)-Mo(1)-Cl(3)	93.5 (2)	Cl(4)-Mo(2)-Cl(5)	86.1 (2)
Cl(2)-Mo(1)-Cl(3)	86.4 (1)	S(1)-Mo(2)-Cl(6)	97.3 (2)
S(1)-Mo(1)-Cl(6)	96.6 (2)	S(2)-Mo(2)-Cl(6)	173.6 (2)
S(3)-Mo(1)-Cl(6)	96.8 (2)	S(3)-Mo(2)-Cl(6)	96.9 (2)
Cl(1)-Mo(1)-Cl(6)	178.1 (2)	Cl(4)-Mo(2)-Cl(6)	89.2 (2)
Cl(2)-Mo(1)-Cl(6)	86.1 (2)	Cl(5)-Mo(2)-Cl(6)	86.5 (2)
Cl(3)-Mo(1)-Cl(6)	88.3 (2)	Mo(1)-S(1)-C(11)	116.3 (6)
Mo(1)-S(1)-Mo(2)	59.7 (1)	Mo(2)-S(1)-C(11)	108.8 (6)
Mo(1)-S(3)-Mo(2)	59.4 (1)	Mo(2)-S(2)-C(21)	113.4 (7)
Mo(1)-S(3)-C(31)	109.4 (5)	Mo(2)-S(3)-C(31)	115.6 (6)
Mo(1)-Cl(6)-Mo(2)	57.7 (1)	Mo(1)-S(3)-Mo(2)	59.4 (1)
Mo(1)-S(1)-Mo(2)	59.7 (1)		

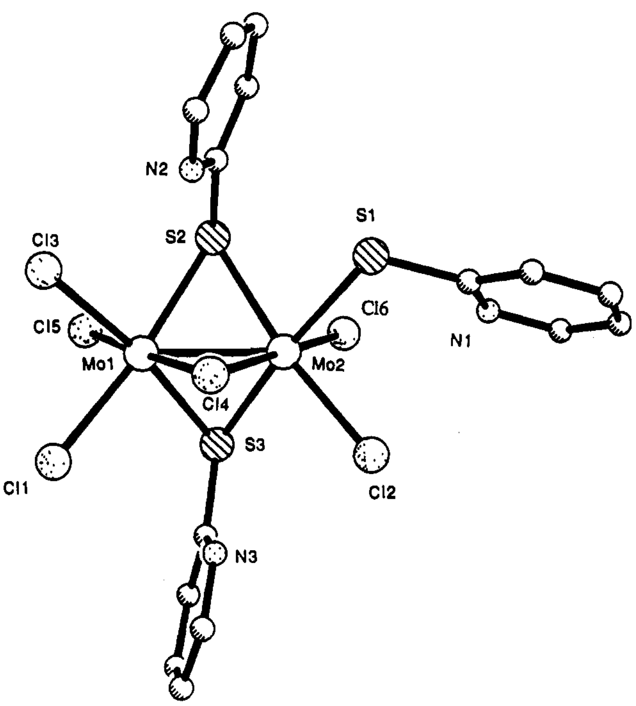

Figure 6. Structure of $[Mo_2Cl_6\{2\text{-}SC_5H_2NH\text{-}3,6\text{-}(SiMe_2Bu^t)_2\}_3]$ (**15**), with the $SiMe_2Bu^t$ groups removed for clarity.

for a Mo(IV) species relative to Mo(III). The Mo–Br and Mo–S distances for the two Mo(III) structures **7** and **8** are statistically equivalent.

The class of binuclear thione-bridged complexes is represented by **14** and **15** shown in Figures 5 and 6, respectively. The binuclear Mo(III) species **14** and **15** are structurally analogous, differing only in the nature and number of organosilyl groups on the thione ligands. The structures consist of discrete binuclear units, exhibiting the confacial bioctahedral geometry common to structures of the $[Mo_2X_9]^{3-}$ class of complexes.[68] In addition to providing unique examples of binuclear Mo(III) complexes with

(68) Cotton, F. A.; Ucko, D. A. *Inorg. Chim. Acta* **1972**, *6*, 161.

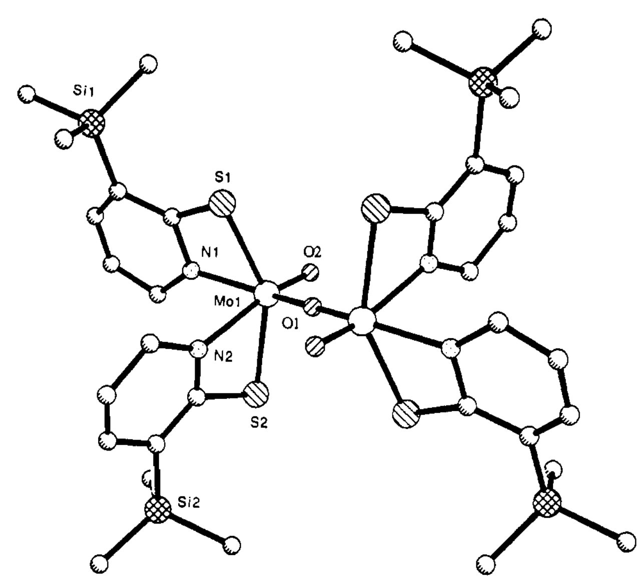

Figure 7. Perspective view of the structure of $[Mo_2O_3(2\text{-}SC_5H_3N\text{-}3\text{-}SiMe_3)_4]$ (**9**).

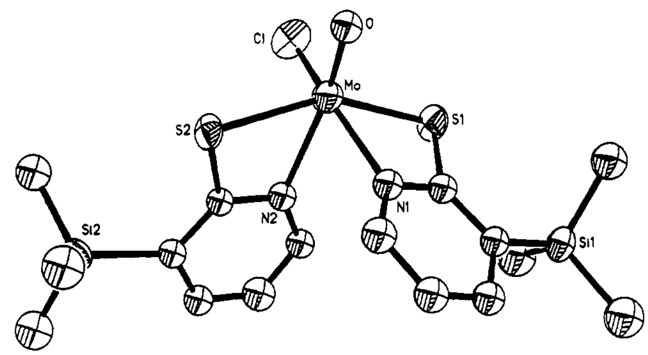

Figure 8. Structure of $[MoOCl(2\text{-}SC_5H_3N\text{-}3\text{-}SiMe_3)_2]$ (**10**).

mixed halido–thione ligand, these complexes exhibit several noteworthy structural features. The three pyridine-2-thiol derived ligands of each structure are all present in the 1*H*-pyridine-2-thione form. The Mo centers are chemically and structurally inequivalent, with one Mo center coordinating to the bridging chloride and thione sulfur donors and to three terminal chlorides while the second Mo site ligates to the bridging chloride and thione sulfur donors, to two terminal chlorides, and to a terminal thione sulfur to give $[MoCl_4S_2]$ and $[MoCl_3S_3]$ coordination geometries, respectively. The Mo–Mo distances, 2.445 (2) and 2.462 (1) Å for **14** and **15**, respectively, are significantly shorter than that observed for the structural prototype $Cs_3[Mo_2Cl_9]$, where the Mo–Mo separation is 2.655 (1) Å.[69] Furthermore, in contrast to the observed paramagnetism of $Cs_3[Mo_2Cl_9]$,[70] **14** and **15** are diamagnetic, a feature also observed for $Cs_3[Mo_2Cl_8H]$ where the Mo–Mo distance is again short, 2.380 (10) Å.[71] This dramatic decrease in the Mo–Mo separation upon substitution of μ-H for μ-Cl in these complex anions has been rationalized on steric grounds. However, a decrease of 0.2 Å upon substitution of μ-S for μ-Cl is unanticipated and must reflect electronic consequences of introducing the thione ligands into the bridge. It is noteworthy that for **14** and **15** the Mo-bridging chloride distances are ca. 0.10 Å longer than the Mo–terminal chloride distances, while the Mo–bridging thione and Mo–terminal thione distances are statistically equivalent. In general, metal–metal distances for the M(III)–M(III) series of confacial bioctahedral structures do not exhibit simple correlations with metal type or bridge ligand identity.[71,72] Other confacial bioctahedral Mo(III) structures with

(69) Saillant, R.; Jackson, P. B.; Streib, W. E.; Folting, K.; Wentworth, R. A. D. *Inorg. Chem.* **1971**, *10*, 1453.
(70) Saillant, R.; Wentworth, R. A. D. *Inorg. Chem.* **1969**, *8*, 1226.
(71) Katovic, V.; McCarley, R. E. *J. Am. Chem. Soc.* **1978**, *100*, 5586.

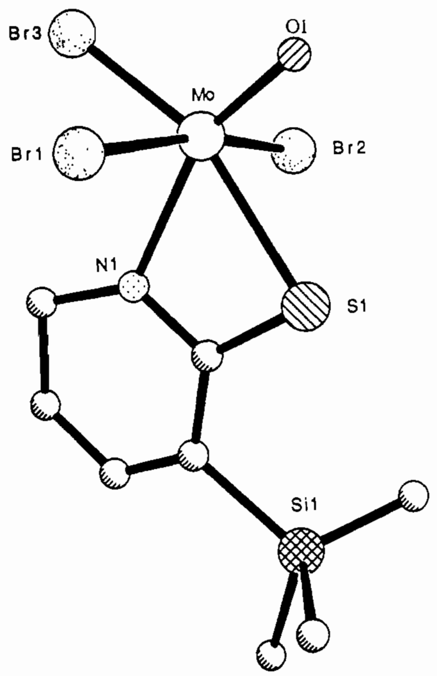

Figure 9. Perspective view of the structure of the molecular anion $[MoOBr_3(2\text{-}SC_5H_3N\text{-}3\text{-}SiMe_3)]^-$ (**11a**).

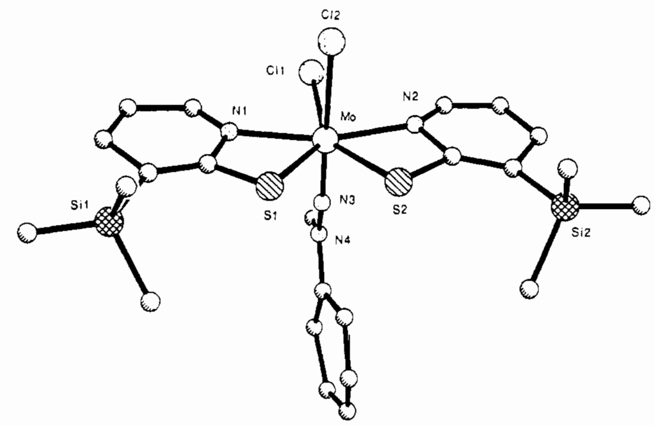

Figure 10. Structure of $[MoCl_2(2\text{-}SC_5H_3N\text{-}3\text{-}SiMe_3)_2(NNMePh)]$ (**12**).

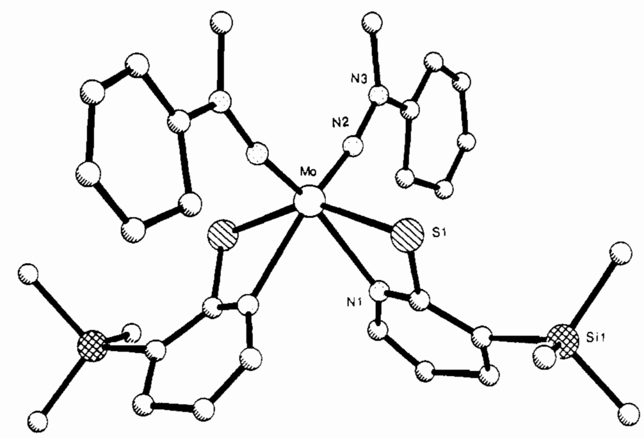

Figure 11. Perspective view of the structure of $[Mo(2\text{-}SC_5H_3N\text{-}3\text{-}SiMe_3)_2(NNMePh)_2]$ (**13**).

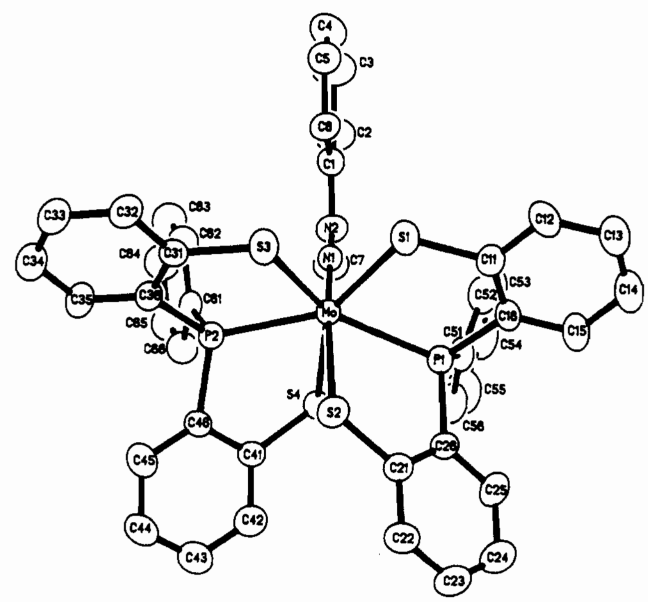

Figure 12. Structure of $[Mo(SC_6H_4PPhC_6H_4S)_2(NNMePh)]$ (**17**).

mixed halido–sulfur donor ligation include $[(Me_2S)Cl_2Mo(\mu\text{-}Cl)_3MoCl_2(SMe_2)]^-$ and $[(Me_2S)Cl_2Mo(\mu\text{-}Cl)_2(\mu\text{-}SMe_2)MoCl_3]^-$.[73]

The structures of the Mo(V)–oxo complexes **9–11** are illustrated in Figures 7–9, respectively. The structure of **9** is unexceptional for a thiolate complex with the common $[Mo_2O_3]^{4+}$ core. Each molybdenum center enjoys distorted octahedral geometry provided by two chelating 3-(trimethylsilyl)pyridine-2-thiolate ligands, the terminal oxo group, and the bridging oxo group, which occupies a crystallographic center of inversion. Thus, the $[Mo_2O_3]$ core exhibits a rigorously planar anti geometry. A similar structure has been reported for $[Mo_2O_3(2\text{-}SC_5H_3N)_4]$,[37] and numerous examples of the $[Mo_2O_3]^{4+}$ have been described.[74,75]

The structure of **9** conforms to the general geometric principles observed for this class of complexes. The nitrogen donors occupy positions trans to the strongly p-bonding oxo groups, thus minimizing competition between the oxo groups and the weakly π-interacting thiolate sulfur donors for the Mo t_{2g} orbitals. As a consequence, the thiolate sulfur atoms are mutually trans, albeit with a grossly distorted angle of 148.6 (1)°. The strong trans influence of the terminal oxo group is evident in the Mo(1)–N(1) distance of 2.328 (5) Å, as compared to the Mo(1)–N(2) distance of 2.199 (5) Å for the nitrogen trans to the less effective bridging oxo group.

The structure of **10** consists of discrete mononuclear units with distorted octahedral geometry about the Mo center as a consequence of ligation by two 3-(trimethylsilyl)pyridine-2-thiolate chelates, an oxo group, and a chloride donor. As expected, a pyridyl nitrogen occupies a positions trans to the oxo group and exhibits the usual bond lengthening. The trans thiolate geometry is similar to that observed for **9** and for $[MoO_2(dibenzo\text{-}1,4,7,10\text{-}tetrathiadecane)]$.[76] Neutral mononuclear Mo(V) complexes with anionic sulfur donors are extremely rare and, although $[MoOCl(dttd)_2]$[76] and $[MoOCl(S_2CNR_2)_2]$[77] have been reported, **10** is the only structurally characterized member of the class.

The structure of the anion of **11** consists of discrete mononuclear units with the Mo center in a distorted octahedral environment provided by the S and N donors of the chelating 3-(trimethylsilyl)pyridine-2-thiolate ligand, three bromide anions and a terminal oxo group. The trans influence of the oxo group is evident in the Mo–N(1) distance of 2.28 (2) Å. Other bond parameters are unexceptional. The bromine ligands assume the meridional orientation, in a fashion similar to that observed for the chloride donors of the analogous $[MoOCl_3(OPPh_3)_2]$.[78] A general geo-

(72) Cotton, F. A.; Kalbacher, B. J. *Inorg. Chem.* **1976**, *15*, 522. Cotton, F. A.; Walton, R. A. *Multiple Bonds Between Metal Atoms*; Wiley-Interscience: New York, 1982.
(73) Boorman, P. M.; Moynihan, K. J.; Oakley, R. T. *J. Chem. Soc., Chem. Commun.* **1982**, 899.
(74) Stiefel, E. I. *Prog. Inorg. Chem.* **1977**, *22*, 1.
(75) Spivack, B.; Dori, Z. *Coord. Chem. Rev.* **1975**, *17*, 99.
(76) Kaul, B. H.; Enemark, J. H.; Merbs, S. L.; Spence, J. T. *J. Am. Chem. Soc.* **1985**, *107*, 2885.
(77) Vasanthi, S.; Nagaraja, K. S.; Udupa, M. J. *Transition Met. Chem. (Weinheim. Ger.)* **1984**, *9*, 382.

Table XII. Selected Bond Lengths (Å) and Angles (deg) for **15**

Mo(1)-Mo(2)	2.462 (1)	Mo(2)-S(1)	2.497 (2)
Mo(1)-S(2)	2.484 (2)	Mo(2)-S(2)	2.467 (2)
Mo(1)-S(3)	2.459 (2)	Mo(2)-S(3)	2.432 (2)
Mo(1)-Cl(1)	2.387 (3)	Mo(2)-Cl(2)	2.434 (2)
Mo(1)-Cl(3)	2.432 (2)	Mo(2)-Cl(4)	2.526 (2)
Mo(1)-Cl(4)	2.533 (2)	Mo(2)-Cl(6)	2.465 (2)
Mo(1)-Cl(5)	2.387 (3)	S(1)-C(11)	1.738 (8)
		S(2)-C(21)	1.775 (8)
		S(3)-C(31)	1.814 (9)
S(2)-Mo(1)-S(3)	98.9 (1)	S(1)-Mo(2)-S(2)	82.8 (1)
S(2)-Mo(1)-Cl(1)	172.6 (1)	S(1)-Mo(2)-S(3)	81.2 (1)
S(3)-Mo(1)-Cl(1)	87.2 (1)	S(2)-Mo(2)-S(3)	100.1 (1)
S(2)-Mo(1)-Cl(3)	85.8 (1)	S(1)-Mo(2)-Cl(2)	92.1 (1)
S(3)-Mo(1)-Cl(3)	174.1 (1)	S(2)-Mo(2)-Cl(2)	171.6 (1)
Cl(1)-Mo(1)-Cl(3)	87.8 (1)	S(3)-Mo(2)-Cl(2)	85.6 (1)
S(2)-Mo(1)-Cl(4)	96.0 (1)	S(1)-Mo(2)-Cl(4)	178.1 (1)
S(3)-Mo(1)-Cl(4)	96.3 (1)	S(2)-Mo(2)-Cl(4)	96.6 (1)
Cl(1)-Mo(1)-Cl(4)	87.5 (1)	S(3)-Mo(2)-Cl(4)	97.2 (1)
Cl(3)-Mo(1)-Cl(4)	86.7 (1)	Cl(2)-Mo(2)-Cl(4)	88.7 (1)
S(2)-Mo(1)-Cl(5)	85.5 (1)	S(1)-Mo(2)-Cl(6)	94.5 (1)
S(3)-Mo(1)-Cl(5)	82.8 (1)	S(2)-Mo(2)-Cl(6)	88.3 (1)
Cl(1)-Mo(1)-Cl(5)	91.1 (1)	S(3)-Mo(2)-Cl(6)	169.9 (1)
Cl(3)-Mo(1)-Cl(5)	94.1 (1)	Cl(4)-Mo(2)-Cl(6)	87.2 (1)
Cl(4)-Mo(1)-Cl(5)	178.4 (1)		
Mo(2)-S(1)-C(11)	117.0 (3)		
Mo(2)-S(2)-Mo(1)	59.6 (1)		
Mo(1)-S(2)-C(21)	109.8 (3)		
Mo(2)-S(2)-C(21)	113.5 (3)		
Mo(1)-S(3)-Mo(2)	60.4 (1)		
Mo(1)-S(3)-C(31)	112.8 (3)		
Mo(1)-Cl(4)-Mo(2)	58.2 (1)		

metric feature of the six-coordinate $[MoO]^{3+}$ core is the occupancy by neutral donors of the position trans to the oxo group, while anionic ligands occupy the equatorial plane. Although a large number of complexes of the general type $[MoOCl_3L_2]$ have been reported,[79-82] the ligands L are invariably neutral, and hence, the complex is likewise unchanged. Complex **11** is, to the best of our knowledge, the first example of an anionic complex with the $[MoOBr_3]$ core.

The hydrazido(2−) class of complexes is represented by compounds **12**, **13**, and **17** shown in Figures 10–12, respectively. The structure of **12** consists of discrete mononuclear units with the Mo center in a distorted pentagonal-bipyramidal geometry. The equatorial plane is defined by the S and N donors of two chelating 3-(trimethylsilyl)pyridine-2-thiolate ligands and one chloride, while the second chloride and the hydrazido(2−) ligand define the axial positions. The hydrazido ligand adopts the common η^1-hydrazido(2−) linear geometry, characterized by short Mo–N(1) and N(1)–N(2) distances and a nearly linear Mo–N(1)–N(2) angle.[83-91] Seven-coordinate Mo–hydrazido and Mo–diazenido complexes have been reported previously, and the pentagonal–bipyramidal geometry is ubiquitous for these species.[56,92-94]

Table XIII. Selected Bond Lengths (Å) and Angles (deg) for **17**

Mo–S(1)	2.524 (2)	Mo–P(1)	2.516 (1)
Mo–S(2)	2.509 (1)	Mo–P(2)	2.499 (1)
Mo–S(3)	2.497 (2)	Mo–N(1)	1.782 (4)
Mo–S(4)	2.578 (1)		
N(1)–N(2)	1.290 (5)		
S(1)–Mo–S(2)	91.9 (1)	S(3)–Mo–P(1)	139.8 (1)
S(1)–Mo–S(3)	66.8 (1)	S(4)–Mo–P(1)	71.8 (1)
S(2)–Mo–S(3)	86.1 (1)	S(1)–Mo–P(2)	142.3 (1)
S(1)–Mo–S(4)	148.8 (1)	S(2)–Mo–P(2)	91.3 (1)
S(2)–Mo–S(4)	81.9 (1)	S(3)–Mo–P(2)	76.0 (1)
S(3)–Mo–S(4)	142.3 (1)	S(4)–Mo–P(2)	68.7 (1)
S(1)–Mo–P(1)	77.1 (1)	P(1)–Mo–P(2)	140.1 (1)
S(2)–Mo–P(1)	78.0 (1)	S(1)–Mo–N(1)	94.4 (1)
S(2)–Mo–N(1)	169.3 (1)	P(1)–Mo–N(1)	95.0 (1)
S(3)–Mo–N(1)	104.3 (1)	P(2)–Mo–N(1)	88.9 (1)
S(4)–Mo–N(1)	88.2 (1)	Mo–N(1)–N(2)	172.1 (4)

Compound **17** illustrates the common features of this structural type and provides another example of this general class. A common geometric feature of the structures is the occupancy of the axial positions by the hydrazido(2−) ligand and by an anionic ligand, chloride or thiolate sulfur. Although it constitutes a common feature of this structural type, the trans thiolate–hydrazido(2−) geometry is generally avoided in five- and six-coordinate complexes.

The structure of **13** conforms to the general structural trends observed for hydrazido(2−) complexes. The Mo center is in a distorted octahedral geometry as a consequence of ligation to the N donors of two linearly coordinated hydrazido(2−) groups, and the S and N donors of two 3-(trimethylsilyl)pyridine-2-thiolate ligands. As anticipated, the pyridine N atoms occupy positions trans to the strongly π-bonding hydrazido groups, requiring the mutually cis orientation of the thiolate S atoms. The cis bis(hydrazido(2−)) geometry has been discussed in detail.[53]

Conclusions

The introduction of sterically encumbering triorganosilyl groups into the pyridine-2-thiol ligand allows the isolation of a series of molybdenum complexes that are otherwise inaccessible. The derivatized ligands serve both to prevent polymerization reactions through bridging thiolate units and to stabilize complexes in a range of molybdenum oxidation states. The thione form of the ligand predominates in the Mo(III) and Mo(IV) oxidation states, while the chelating thiolate form is observed for Mo(V) and Mo(VI) complexes. The range of oxidation states of the molybdenum and the variety of coligands incorporated into the various structural types illustrate the remarkable versatility of this ligand type.

Acknowledgment. This work was supported by the National Institute of Health (Grant GM22566 to J.Z. and E.B.), the National Science Foundation, the donors of the Petroleum Research Fund, administered by the American Chemical Society, and Societe Nationale Elf Aquitaine (E.B.). We also thank the National Science Foundation for funding for the purchase of NMR spectrometer.

Supplementary Material Available: For 12 structures, ORTEP plots and tables of crystallographic data, atomic positional parameters, bond lengths and angles, calculated hydrogen atom positions, and anisotropic temperature factors (88 pages); tables of calculated and observed structure factors (198 pages). Ordering information is given on any current masthead page.

(78) Garner, C. D.; Howlander, N. C.; Mabbs, F. E.; McPhail, A. T.; Onan, K. A. *J. Chem. Soc., Dalton Trans.* **1978**, 1848.
(79) Walton, R. A. *Prog. Inorg. Chem.* **1972**, *16*, 1.
(80) Edwards, D. A. *J. Inorg. Nucl. Chem.* **1965**, *27*, 303.
(81) Mitchell, P. C. H. *J. Inorg. Nucl. Chem.* **1963**, *25*, 963.
(82) Horner, S. M.; Tyree, S. Y. *Inorg. Chem.* **1962**, *1*, 122.
(83) Bishop, M. W.; Chatt, J.; Dilworth, J. R.; Hursthouse, M. B.; Motevalle, M. *J. Chem. Soc., Dalton Trans.* **1979**, 1600.
(84) Takahashi, T.; Mizobe, Y.; Sato, M.; Uchida, Y.; Hidai, M. *J. Am. Chem. Soc.* **1980**, *102*, 7461.
(85) Heath, G. A.; Mason, R.; Thomas, K. M. *J. Am. Chem. Soc.* **1974**, *96*, 259.
(86) Gebreyes, K.; Zubieta, J.; George, T. A.; Koczon, L. M.; Tisdale, R. C. *Inorg. Chem.* **1986**, *25*, 407.
(87) Bultitude, J.; Larkworthy, L. F.; Povey, D. C.; Smith, G. W.; Dilworth, J. R.; Leigh, G. J. *J. Chem. Soc., Dalton Trans.* **1986**, 1748.
(88) Dilworth, J. R.; Morton, S. *J. Organomet. Chem.* **1986**, *314*, C25.
(89) Shaikh, S. N.; Zubieta, J. A. *Inorg. Chem.* **1986**, *25*, 4613.
(90) Bishop, P. T.; Dilworth, J. R.; Morton, S.; Zubieta, J. A. *J. Organomet. Chem.* **1988**, *341*, 373.
(91) Nicholson, T. J.; Zubieta, J. *Polyhedron* **1988**, *7*, 171 and references therein.
(92) Butler, G.; Chatt, J.; Leigh, G. J.; Smith, A. R. P.; Williams, G. *Inorg. Chim. Acta* **1978**, *28*, 165.
(93) March, F. C.; Mason, R.; Thomas, K. K. *J. Organomet. Chem.* **1975**, *96*, C43.
(94) Chatt, J.; Dilworth, J. R.; Dahlstrom, P.; Zubieta, J. *J. Chem. Soc., Chem. Commun.* **1980**, 786.
(95) Figuly, G. D.; Loop, C. K.; Martin, J. C. *J. Am. Chem. Soc.* **1989**, *111*, 654.
(96) Block, E.; Gernon, M.; Kang, H.; Liu, S.; Zubieta, J. *Inorg. Chim. Acta* **1990**, *167*, 143.